

Techno-economic analysis of the impact of working fluids on the concentrated solar power combined with multi-effect distillation (CSP-MED)

A.M. Soliman^{a,b}, Abdelnasser Mabrouk^{b,c}, Mohamed A. Sharaf Eldean^{b,*}, Hassan E.S. Fath^d

^aMechanical Engineering Department, Faculty of Engineering, Jouf University, Sakaka, Saudi Arabia, email: amsoliman@ju.edu.sa

^bDepartment of Mechanical Engineering, Faculty of Engineering, Suez University, Suez, Egypt, Tel. +601139795943; emails: mohammed.eldeen@suezuniv.edu.eg/mwahab31@yahoo.com (M.A. Sharaf Eldean), aaboukhlewa@hbku.edu.qa (A. Mabrouk)

^cQatar Environment and Energy Research Institute, Hamad Bin Khalifa University, Qatar Foundation, Doha, Qatar

^dEgypt–Japan University of Science and Technology, Alexandria, Egypt, Tel. +00201271111740; emails: h_elbanna_f@yahoo.com/hassan.fath@ejust.edu.eg

Received 15 January 2020; Accepted 14 September 2020

ABSTRACT

Concentrated solar power (CSP) is considered a vital option for thermal desalination processes. Furthermore, power generation is an excessive option to be produced. In this work, thermo-economic analysis of the concentrated solar power combined with multi-effect distillation process at different working fluids has been performed. The first configuration is about utilizing the water steam Rankine cycle, while the second configuration is about the organic Rankine cycle (ORC). The main concept is to desalinate seawater and to produce electricity. Parabolic trough collector (PTC) is used as the main source of thermal power collection. Molten salt (MS) working fluid is used for the first configuration, while Therminol-VP1 heat transfer oil is considered for the ORC configuration. Thermo-economic scenarios based on the variation of operating conditions, exergy, and cost analysis are performed to evaluate the proposed system according to the unit product cost, \$/GJ, and the hourly cost, \$/h. The results reveal that the power generation scenario is thermo-economically effective by generating 100 MWe with 3.5 \$/GJ. According to the simulation results, solar ORC configuration gives attractive results against the solar steam Rankine cycle based on thermo-economic product cost (14 vs. 19 \$/GJ), total hourly costs (205 vs. 704.5 \$/h), power cost (0.027 vs. 0.042 \$/kWh), and water price (0.9 vs. 1.12 \$/m³).

Keywords: Thermo-economic; Multi-effect distillation; Solar organic cycles; Power generation

1. Introduction

Water is available in abundant quantities in nature; however, there is a shortage of potable water in some places of many countries in the world. Desalination seems to be the most suitable solution. However, desalination technologies are considered insatiable to power consumption. To support the desalination plant, a dominant source of power should be

adopted and usually be a fossil fuel. However, environmental pollution and energy crisis have been considered the worldwide key topic and that developing clean energy and improving energy efficiency are of great significance to alleviate the crisis. The world's energy demand, in fact, is nowadays growing more and more and the problem of fossil fuels depletion is becoming increasingly crucial. It is also important to consider that currently more than 25 billion tons of

* Corresponding author.

CO₂ arising from worldwide human activities are released annually into the atmosphere. For that reason, the development of new “green technologies” such as concentrated solar power (CSP) is a stringent necessity, both to meet the energy demands and to limit the production of carbon dioxides, carbon monoxide, and particulate matter. Besides, nowadays renewable energy sources characterized by low temperatures and low heat values have appealed increasing interest owing to their high accessible amounts for exploitation. Moreover, water shortage problem is considered a huge problem around the worldwide. Ironically, places with water shortages almost have a plenty of solar energy such as north Africa region and the gulf area of middle east region. Therefore, solar desalination is considered one of the best options that should be utilized for freshwater production [1]. Considering Egypt as an example that representing the MENA region, the tourist sector in Egypt is in the development process and it would consume huge amounts of energy and surly freshwater especially in the Red Sea and north coast regions. At the same time, solar energy is massively available (Egyptian sunshine hours almost equal to 3,600 h [2]) in that mentioned regions with no existence of freshwater. Therefore, solar thermal desalination technology could be considered as the main player for such cases of development, especially in the tourist sector. Thermal and/or electrical desalination technologies such as reverse osmosis (RO), multi-stage flash (MSF), multi-effect distillation (MED), thermal vapor compression (MED-TVC), and mechanical vapor compression (MED-MVC) can be effectively combined with solar power plants [3–7]. It can power these different desalination techniques by providing the required electricity via photovoltaic (PV) and/or concentrating solar power (CSP) [8,9]. Among the several options of the connection between the desalination systems and the solar power plant, the combination of MED and a solar trough field is considered one of the most promising techniques. Therefore, the race for the second generation of the seawater desalination systems has been settled between reverse osmosis (RO) and low-temperature MED of horizontal tube evaporators [10]. Both systems are characterized by their low energy consumption as compared to the MSF system [11]. Conventional MED desalination process uses about half of the MSF pumping energy, and almost the same amount of thermal energy used by the MSF, if both have the same gain ratio [12]. However, a recent trend of using low-temperature MED allows the use of low temperature (in the range of 70°C) steam as a heat source, and consequently of low exergy and low equivalent work. This can bring the MED mechanical energy consumption close to the consumption of the efficient RO system. There are many research activities about the MED operation and performance. For example, a construction in Abu Dhabi of MED plant with a 240,000 m³/d capacity shows a breakthrough in large-scale MED plants [13]. Askari et al. [14,15] compared thermo-economically between the freshwater costs of the dual purpose linear Fresnel rankine cycle with MED plants and the case when the MED and MED-TVC systems use direct steam of the linear Fresnel solar field (LFC) to produce fresh water. Askari et al. [15] results show that the freshwater costs of the LFC/MED and LFC/MED/TVC configurations are higher than that of the dual-purpose plants. The gain ratio value was ranged between 9 and 12 at a steam temperature around

70°C. In the same regard, Alhaj et al. [16] studied the combination between LFC and MED process. The results showed that 1 m² of solar linear Fresnel collector produces 8.6 m³ of freshwater per year. The equivalent mechanical energy of the optimized MED desalination plant was 8 kWh/m³, which is 59% lower than that of existing commercial MED facilities with thermal vapor compression (19 kWh/m³). Samson et al. [17] analyzed the possibility of using steam accumulators as buffer storage indirect steam generation for solar MED thermal vapor compression. Moreover, Casimiro et al. [18] simulated the CSP plant working in cogeneration with a low-temperature MED with parallel feed (MED-PF) configuration. Casimiro analysis shows that MED-PF configuration gives attractive results against the thermal vapor compression (MED-TVC). Bandelier et al. [19] analyzed the possibilities of using low-grade solar heat for the MED desalination process. Coupling low-temperature MED with a solar heat source downstream of a CSP power plant allows being benefitting of a low marginal cost heat source. Yang et al. [20] analyzed exergetically the possibilities of using a flat plate collector (FPC) as a low source of heat with the MED desalination process. Yang’s analysis suggested that to increase the steam temperature to improve the exergy efficiency. Palenzuela et al. [21] studied a 72 m³/d pilot low-temperature MED plant located at the Plataforma Solar de Almería, Spain. The performance ratio reached its maximum when the last effect vapor temperature ranged from 25°C to 35°C since the temperature difference between effects was lower. Regarding to lower temperature operation, organic Rankine cycle (ORC) can play an active and vital rule in that situation. ORC could utilize the low-medium temperature heat to generate and thus improve the energy utilization efficiency. As mentioned earlier, it would be quite attractive to combine between renewable energy and desalination technologies for that purpose. However, a general overview about global energy consumption should be performed in this regard. Sharaf et al. [11], Sharaf [22], and Sharaf Eldean and Soliman [24] analyzed thermo-economically many of solar desalination processes. That study was about the possibility of combining SORCs with thermal desalination processes. Sharaf studies [11,22–24] revealed that it is possible and feasible to combine such processes to each other especially for the solar MED. Solar organic Rankine cycle (SORC) for MED proved that parallel feed configuration is dominant against the other configurations. For direct vapor generation, Iodice et al. [25,26] studied the use of direct vapor generation from the solar thermal PTC through the steam Rankine cycle. Steam screw expander has been adopted in Iodice’s work [25,26]. The system overall efficiency was in the range of 7.7%–12.6%. Liang et al. [27] addressed the simultaneous optimization of a combined supercritical CO₂ Brayton cycle. ORC was integrated with molten salt solar power tower plant. The ORC was added as a bottoming cycle to recover the waste heat of the Brayton cycle to generate extra power. Oyekale et al. [28,29] investigated the optimization potentials in a conceptual hybrid solar-biomass ORC cogeneration plant, through component-based exergy and exergo-economic analyses. The ORC was rated at 629 kWe, and it was related to a real and operational plant. Another CSP work for solar MED (MATS Project) has been established in Borg El-Arab city, Alexandria, Egypt [30–32]. MATS project was a desalination

plant powered by CSP technology for 250 m³/d, and 1 MWe of electric power generation. The project was a real feasible desalination plant that demonstrates the possibility of coupling the solar thermal power cycles with MED process. Related to the same topic of optimization and thermo-economic analysis, Khamis Mansour et al. [31] studied computationally the vapor flow shapes through the MED stages or effects. Computational fluid dynamic (CFD) analysis was performed in Khamis Mansour et al. [31] work. Khamis work was performed regarding MATS project concept.

In this work, thermo-economic evaluation of CSP powered MED desalination process is performed according to two main configurations of MATS concept. The first one is the solar steam Rankine cycle (SSRC), and the second is the SORC. The first part of this paper presents the defect of the first configuration (MATS concept) as a reference, and accordingly address the solution by applying the second configuration (SORC). The following criteria are considered in this study:

- MATS project concept will be considered in this work as a reference to optimize the operating conditions.
- CSP combined with MED parallel feed configuration is thermo-economically evaluated.
- Energy, exergy, and cost analysis will be performed for the proposed system. Optimized operating conditions will be assigned based on thermo-economic terms. Therefore, SORC [33] for MED will be compared against the reference system (MATS project concept [30–32]).
- Dynamic modeling is presented based on different operating conditions.

2. MATS project concept

The MATS project “Multipurpose Applications by Thermodynamic Solar,” co-funded by the European Union under the seventh Framework Program. The project aims to demonstrate secure production of electrical power and water supply for a community of at least 1,000 people in a desert area, through the following main steps:

- Solar energy is captured and stored at elevated temperature heat, to generate superheated steam to drive a thermo-electrical steam cycle.
- Electrical power production is combined with a desalination unit using residual heat to produce freshwater from salty water. This way, it will be possible to generate electricity and co-generate fresh water in a desert region, supporting the social, and economic growth of the area.

The MATS Consortium includes partners from Italy, Egypt, France, Germany, and the UK. The lead partner of the Project is the Italian National Agency for new technologies, energy, and sustainable economic development (ENEA). The lead Egyptian research partner is the Academy of Scientific Research and Technology (ASRT) in Egypt. The total budget of the project is 22.0 million Euros. MATS CSP plant has been built inside the City for Science and Technology (SRTA-City) in Borg El-Arab. The plant is the first of its kind in the world with its unique features of environmentally friendly fluids, easy management, and

flexibility of operation. MATS technology is based on linear parabolic mirrors that concentrate the solar radiation to generate heat at high temperatures. Solar receiver tubes absorb the concentrated solar radiation and the heat is transferred to a heat transfer fluid. The innovative solar technology proposed in MATS makes use of molten salts (sodium and potassium nitrates) as the heat transfer fluid. That fluid has several positive environmental, safety, and technical features, including the possibility to operate at low pressures and reach temperatures as high as 550°C. The solar collectors, back-up heater, and heat storage system were individually developed with prototypes tested at ENEA (Italy). The system allows the controlled production of super-heated steam, which drives a steam cycle for electrical power generation. Moreover, a co-generative power cycle is designed with a MED applied as the steam condenser unit, to recover the residual heat from the exhaust stream. Fresh desalinated water represents a high-value by-product, especially in CSP plants built in desert areas with water shortage. Heating and cooling of buildings represent another co-generation option. The MATS plant includes 18 solar collectors, each 100 m long, with a total reflective panel area of 10,000 m². During normal operation, molten salts enter the solar field at 290°C, collect solar energy, and are heated up to 550°C. Molten salts are collected in a heat storage tank integrated with a steam generator. Produced steam (460°C, 55 bar) feeds a co-generative cycle to produce 1 MWe power with 250 m³/d of desalinated water from the MED unit. The plant is well-integrated with the local energy and water cycles: it is connected with local gas and electrical utility grids; furthermore, the plant is also linked with the local water cycle as raw water extracted from wells is purified and high-quality water produced for different local market uses. Fig. 1 shows the schematic diagram of MATS project concept.

The proposed plant has consisted of two parts: (i) solar part and (ii) steam Rankine cycle (SRC) part. The main plant units are summarized as following:

- Solar parabolic trough collector (PTC) with molten salt working fluid. PTC is responsible about transferring solar heat generation to the boiler heat exchanger (BHX) (storage) tank. BHX with the entire pumping system for molten salt circulation as a hot side. Cold side will be represented as water steam working fluid. The power block which contains steam turbine unit and electric generator for electric power generation.
- Two units of MED-parallel feed configuration (MED-PF) for dual purpose (desalination and condensation). Pumping system (feed, brine, and distillate pumps) is contained within the MED-PF plant.
- Pumping unit for the steam Rankine cycle (SRC) side for recirculation and pressure loss overcoming.

3. Thermo-economic model

In this part, the proposed system is mathematically analyzed to be evaluated it using thermo-economic approach (exergy and cost). Exergy and thermo-economic analyses are performed according to the embedded equations in the SDS-REDS software package [23,24,34]. Thermo-economic is the branch of engineering that combines exergy analysis

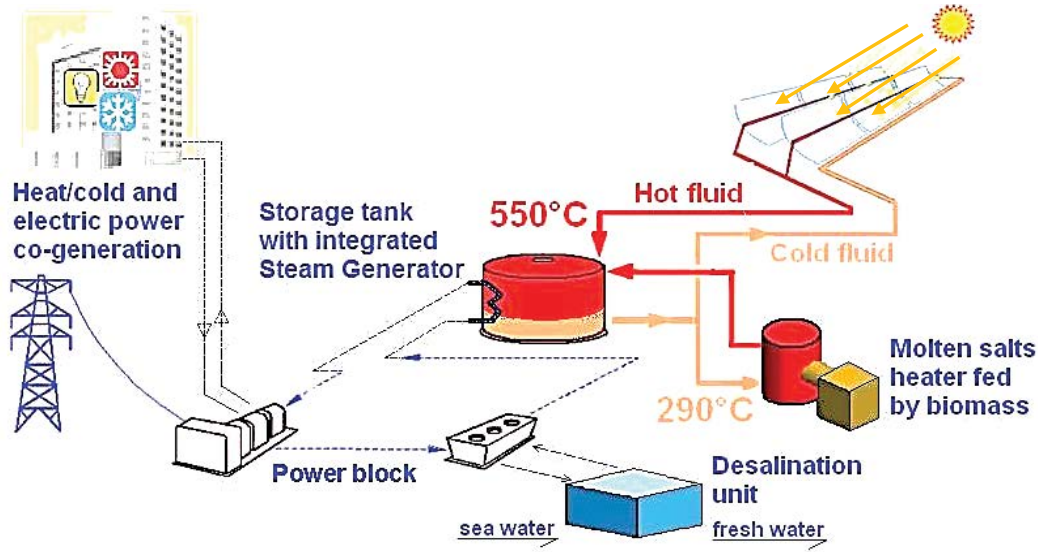


Fig. 1. Schematic diagram of MATS project concept of CSP assisted MED for desalination and power generation.

and cost principles to provide the system designer or operator with information not available through conventional energy analysis and economic evaluations [35,36]. Thermo-economic balance for any unit is performed based on exergy and cost balances. In a conventional economic analysis, a cost balance is usually formulated for the overall system operating at steady state as following [35,36]:

$$\sum_{\text{out}} \dot{C} = \sum_{\text{in}} \dot{C} + Z^{\text{IC\&OM}} \quad (1)$$

where \dot{C} is the cost rate according to inlet and outlet streams, and $Z^{\text{IC\&OM}}$ is the capital investment and operating and maintenance costs. In exergy costing a cost is associated with each exergy stream. Thus, for inlet and outlet streams of matter with associated rates of exergy transfer $E_{i,o}$, power W , and the exergy transfer rate associated with heat transfer E_q it can write as following:

$$\dot{C}_{i,o} = c_{i,o} \dot{E}_{i,o} \quad (2)$$

$$\dot{C}_w = c_w \dot{W} \quad (3)$$

$$\dot{C}_q = c_q \dot{E}_q \quad (4)$$

where $c_{i,o,w,q}$ denote average costs per unit of exergy in \$/kJ for inlet (i), outlet (o), power (w), and energy (q), respectively. Thermo-economic main terms based on [24] are assigned as following:

- The cost of power is assigned based on the price of the electricity 0.06\$/kWh [25].
- The specific power cost would become 0.06/3,600 \$/kJ.

3.1. Exergy analysis

Unlike energy, which is conserved in any process according to the first law of thermodynamics, exergy is destroyed

due to irreversibility taking place in any process, which manifests itself in entropy creation or entropy increase. The exergy analysis is performed based on thermodynamic potential exergy, which considers the energy as well as its potential use (quality). In outline, the exergy analysis of the proposed processes will be implemented based on the following terms:

- The processes are in steady-state condition.
- Chemical and physical exergy components are performed for each stream in desalination plant.
- The negative exergy rate of blow-down represents the potential use of rejected chemical exergy with respect to seawater. Commonly, this potential use is wasted in desalination facilities where rejected brine is merely returned to the sea. Then, this loss of exergy represents the impact of waste on the surroundings.

The general form of the exergy is defined by the following equation:

$$Ex_2 - Ex_1 = Ex_q + Ex_w + Ex_{fi} - Ex_{fo} - \dot{I} \quad (5)$$

where $Ex_2 - Ex_1 = 0$ is the non-flow exergy change in steady-state condition, $Ex_q = \sum_j (1 - T_{\text{amb}}/T_j) \times Q_j$ is the exergy transfer due to the heat transfer between the control volume and its surroundings, $Ex_w = -W_{\text{cv}} + P_o(V_2 - V_1)$ is equal to the negative value of the work produced by the control volume but in most cases, the control volume has a constant volume, therefore Ex_w can be further simplified. $I = T_{\text{amb}} \times S_{\text{gen}}$ is the exergy destruction in the process. The flow availability expressed as $Ex_{fi,o} = \sum_{i,o} \dot{m}_{i,o} e_{fi,o}$. Hence, the general form in steady-state condition would become:

$$0 = Ex_q + Ex_w + Ex_{fi} - Ex_{fo} - \dot{I} \quad (6)$$

The exergy destruction rate (kW) in solar collector is obtained by [37] as:

$$\dot{I}_{\text{collector}} = A_{\text{col}} \times G_b \times \left(1 + \frac{1}{3} \left(\frac{T_{\text{amb}}}{T_{\text{sun}}} \right)^4 - \frac{4}{3} \left(\frac{T_{\text{amb}}}{T_{\text{sun}}} \right) \right) + \dot{m}_{\text{col}} [h_i - h_o - T_{\text{amb}} (s_i - s_o)] \quad (7)$$

Nafey et al. [30] has recommended $T_{\text{sun}} = 6,000$ K and this value is used in this study.

$$\dot{I}_{\text{turbine}} = \dot{m} [\Delta h_{i-o} - T_{\text{amb}} \times \Delta s_{i-o}] - \dot{W}_{\text{turbine}} \quad (8)$$

$$\dot{I}_{\text{rec,cond}} = \dot{m}_{\text{hot}} [\Delta h_{i-o} - T_{\text{amb}} \times \Delta s_{i-o}]_{\text{hot}} + \dot{m}_{\text{cold}} [\Delta h_{i-o} - T_{\text{amb}} \times \Delta s_{i-o}]_{\text{cold}} \quad (9)$$

$$\dot{I}_{\text{pump}} = \dot{m} [\Delta h_{i-o} - T_{\text{amb}} \times \Delta s_{i-o}] + \dot{W}_{\text{pump}} \quad (10)$$

$$\dot{I}_{\text{MED}} = \Delta E \dot{x}_{\text{steam}} + \dot{W}_{\text{pumps}} - E \dot{x}_f - E \dot{x}_b - E \dot{x}_d \quad (11)$$

where $E \dot{x}_f$ represents the chemical and physical exergy of seawater feed stream to the MED effects, $E \dot{x}_b$ is the exergy stream associated with brine and neglected as loss stream, while $E \dot{x}_d$ is the chemical and physical exergy stream of distillate product, and $\Delta E \dot{x}_{\text{steam}}$ is the exergy stream of steam conditions based on inlet and outlet cases.

Exergy of saline streams is obtained based on physical and chemical components. For physical part, the exergy streams for feed, brine, and distillate are functions of h_f , h_b , and h_d which are calculated based on seawater specific heat capacity C_p , salinity s , and feed seawater temperature for each stream [38] where:

$$h_{f,d,b} = h_o + \left(A \times T + \frac{B}{2} \times T^2 + \frac{C}{3} \times T^3 + \frac{D}{4} \times T^4 \right) \quad (12)$$

where $h_o = 9.6296 \times s - 0.4312402 \times s^2$ and $A = 4,206.8 - 6.6197 \times S + 1.2288 \times 10^{-2} \times S^2$, $B = -1.1262 + 5.4178 \times 10^{-2} \times S - 2.2719 \times 10^{-4} \times S^2$, $C = 1.2026 - 5.3566 \times 10^{-4} \times S + 1.8906 \times 10^{-6} \times S^2$, $D = 6.8774 \times 10^{-7} + 1.517 \times 10^{-6} \times S - 4.4268 \times 10^{-9} \times S^2$

Therefore, the physical exergy equation (kg/s) for any saline stream is obtained as:

$$E \dot{x}_{\text{ph}} = \dot{m} \left(C_p (T, S) \times (T - T_o) \times C_p (T, S) \log \frac{T}{T_o} \right), \quad (T_o = \text{reference temperature}) \quad (13)$$

For chemical part, the exergy stream (kg/s) should be calculated according to the following relation:

$$E \dot{x}_{\text{ch}} = \dot{m} \left(\frac{N_{\text{mol}} (S, M_w, M_s) \times 10^{-3} \times 8.314 \times}{T_o} \left\{ -X_w \times \log X_w - X_s \times \log X_s \right\} \right) \quad (14)$$

Total stream exergy rate is then calculated:

$$E \dot{x}_{\text{total}} = E \dot{x}_{\text{ph}} + E \dot{x}_{\text{ch}} \quad (15)$$

where,

$$X_w = \frac{N_{\text{pure}} (S, M_w)}{N_{\text{mol}} (S, M_w, M_s)} \quad (16)$$

$$X_s = \frac{N_{\text{salt}} (S, M_w)}{N_{\text{mol}} (S, M_w, M_s)} \quad (17)$$

$$N_{\text{pure}} = \frac{1,000 - S}{M_w} \quad (18)$$

$$N_{\text{salt}} = \frac{S}{M_s} \quad (19)$$

where $N_{\text{mol}} = N_{\text{pure}} + N_{\text{salt}}$ is the number of particles, and X_w , X_s is the fraction of water and salt (mol), and the molar weight $M_{w,s}$ for water and salt is 18 and 58.5 g, respectively. The overall exergy efficiency that considered in this study is performed based on the following relation:

$$\eta_{\text{ex}} = 1 - \frac{\dot{I}_{\text{total}}}{E \dot{x}_{\text{in}}} \quad (20)$$

3.2. Thermo-economic analysis

For cost analysis, investment and operating and maintenance costs analyses are performed for each component, solar field, steam turbine, boiler heat exchanger (BHX), MED, and pump units. The main assumptions for cost analysis are outlined as following:

- The interest rate and set as 5%.
- LT_p is the plant lifetime and set as 20 y.
- Tables 1 and 2 illustrate the ICC and O&M costs for the cycle components.
- Cost of brine blow-downstream is set as zero costs [33].

Investment and operating and maintenance costs analyses are performed for each component, solar field, steam turbine, recuperator, BHX, and pump units. The interest rate and set as 5%, LT_p is the plant lifetime and set as 20 y. Tables 1 and 2 illustrate the ICC and O&M costs for the cycle components. Table 1 shows the costs for solar field, steam turbine, condensers, and pump unit. Cost analysis is varying according to each unit and market share prices. For the MED part, cost analyses are estimated based on direct capital costs (DCC) and the total capital costs (TCC).

The cost stream equation from pump unit to solar collector should become as:

$$C_{\text{pump-col}} = C_w + C_{\text{bhx-pump}} + Z_{\text{pump}}^{\text{IC\&OM}} \quad (21)$$

where C_w is the power cost, \$/kJ, and $C_{\text{bhx-pump}}$ parameter are the cost stream from the BHX unit toward the pump, and Z_{pump} is the pump hourly cost, \$/h. So, the unit product cost, \$/kJ for the pump will be calculated as:

$$C_{\text{pump-col}} = \frac{C_w E \dot{x}_w + C_{\text{bhx-pump}} E \dot{x}_{\text{bhx-pump}} + Z_{\text{pump}}^{\text{IC\&OM}}}{E \dot{x}_{\text{pump-col}}} \quad (22)$$

Table 1
ICC and O&M costs for solar Rankine cycle components

Parameter	ICC, \$	O&M, \$	TCC, \$/y	$Z^{IC\&OM}$, \$/h	Reference
Solar collector	$150 \times (A_{col})^{0.95}$	$15\% \times ICC_{col}$	$A_f \times (ICC + O\&M)_{col}$	$TCC_{col}/8,760$	[36]
Steam turbine	$4,750 \times (W_t)^{0.75}$	$25\% \times ICC_t$	$A_f \times (ICC + O\&M)_t$	$TCC_t/8,760$	[36]
Steam generator	$150 \times (A_{cond})^{0.8}$	$25\% \times ICC_{cond}$	$A_f \times (ICC + O\&M)_{cond}$	$TCC_{cond}/8,760$	[36]
Pump	$3,500 \times (W_p)^{0.47}$	$25\% \times ICC_p$	$A_f \times (ICC + O\&M)_p$	$TCC_p/8,760$	[36]
Storage HEX	$500 \times \text{Volume}$	$15\% \times ICC_{stg}$	$A_f \times (ICC + O\&M)_{stg}$	$TCC_{stg}/8,760$	[39]

Table 2
Cost parameters for MED-PF desalination plant

Parameter	Correlation	Reference
Interest rate, %	5	
Plant life time, y	20	[33]
Amortization factor, 1/y	$A_f = \frac{i(1+i)^{LT_p}}{(1+i)^{LT_p} - 1}$	[40]
Direct capital costs, \$	$DCC = 9 \times 10^5$	[40]
Annual fixed charges, \$/y	$AFC = A_f \times DCC$	[40]
Annual heating steam costs, \$/y	$AHSC = \frac{SHC \times L_s \times LF \times M_d \times 365}{1,000 \times PR}, \quad SHC = \frac{1.466\$}{MkJ}$	[40]
Annual electric power cost, \$/y	$AEPC = SEC \times SPC \times LF \times M_d \times 365, \quad SEC = 0.06\$/kWh$	[40]
Annual chemical cost, \$/y	$ACC = SCC \times LF \times M_d \times 365, \quad SCC = 0.025\$/m^3$	[40]
Annual labor cost, \$/y	$ALC = SLC \times LF \times M_d \times 365, \quad SLC = 0.1\$/m^3$	[40]
Total annual cost, \$/y	$TAC_{MED} = AFC + AHSC + AEPC + ACC + ALC$	[40]
Operating and maintenance costs, \$	$OMC_{MED} = 0.02 \times DCC$	[40]
Hourly operating and maintenance costs, \$/h	$Z_{MED}^{IC\&OM} = \frac{OMC_{MED} \times A_f + AFC}{8,760}$	[40]
Total plant costs, \$/y	$TPC = TCC_{col} + TCC_{bhx} + TCC_{rec} + TCC_p + TCC_t + TAC_{MED}$	[40]
Total water price, \$/m ³	$TWP = \frac{TPC}{(D_p \times 365 \times LF)}$	[40]

where Ex_w is the exergy of the pumping power, kW, $Ex_{bhx-pump}$ is the exergy stream from BHX to the pump unit, kW and $Ex_{pump-col}$ is the exergy flow stream from the pump to the solar collector. For the solar collector unit, the relation would be calculated based on input and output streams like following:

$$C_{col-bhx} = C_q + C_{pump-col} + Z_{col}^{IC\&OM} \quad (23)$$

where C_q is the cost of heat transfer to the solar collector, $C_{pump-col}$ is the cost stream from Eq. (22), and Z_{col} is the collector hourly cost parameter, \$/h. The product cost rate, \$/kJ from solar collector field to the BHX unit is then calculated as following:

$$C_{col-bhx} = \frac{C_{p-col} Ex_{p-col} + Z_{col}^{IC\&OM}}{Ex_{col-bhx}} \quad (24)$$

where Ex_{p-col} is the exergy flow from the pump unit to the solar field, kW, and $Ex_{col-bhx}$ is the exergy flow from the solar collector to the BHX unit, kW. The thermo-economic balance for BHX unit is calculated as:

$$C_{bhx-med} + C_{bhx-pump} = C_{col-bhx} + C_{med-bhx} + Z_{bhx}^{IC\&OM} \quad (25)$$

where $C_{bhx-med}$ is the cost stream toward the MED unit, $C_{bhx-pump}$ is the outlet cost stream to the pump (toluene in case of ORC), $C_{col-bhx}$ is the cost stream from the solar

collector to the BHX unit (therminol-VP1), and $C_{med-bhx}$ is cost stream from the MED back to the BHX unit.

The unit product cost stream from BHX to the condenser unit is performed as:

$$C_{bhx-med} = \frac{C_{med-bhx} Ex_{med-bhx} + Z_{bhx}^{IC\&OM}}{Ex_{bhx-pump}} \quad (26)$$

where $C_{bhx-pump} = C_{col-bhx}$, and Ex is the exergy stream in kW. In case of use recuperator unit (SORC):

$$C_{rec-bhx} + C_{rec-med} = C_{st-rec} + C_{p-bhx} + Z_{rec}^{IC\&OM}, C_{rec-bhx} = C_{p-bhx} \quad (27)$$

where $C_{rec-bhx}$ is the cost stream from the recuperator unit back toward to the BHX for regeneration, $C_{rec-med}$ is the cost stream from the recuperator toward the MED unit, and C_{st-rec} is the cost stream from the steam turbine towards the recuperator. For the MED process streams:

$$C_d + C_{brine} + C_{steam-p} = C_{steam-med} + C_{fi} + Z_{med}^{IC\&OM} \quad (28)$$

where C_d is the distillate product cost \$/h, C_{brine} is the brine blowdown cost and is specified as zero cost, and C_{fi} is the inlet feed stream cost is calculated based on the following analysis [25,33]. For chemical cost and dosing rate, the sulfuric acid = 0.504 \$/kg, sulfuric dose rate = 24.2 g/ton of the makeup water. The caustic acid = 0.701\$/kg and caustic dose rate = 14 g/ton of makeup water. For anti-scalant = 1.9 \$/kg, and the anti-scalant dose rate = 4 g/ton of the makeup water. The chlorine = 0.48 \$/kg and chlorine dose rate = 4 g/ton of makeup water. Therefore, the total feed cost rate \$/h can be calculated from the following relation:

$$C_f = M_f \times \left(\begin{array}{l} \text{sulfuric acid} \times \text{sulfuric dose rate} + \text{caustic acid} \times \\ \text{caustic dose rate} + \text{anti-scalant} \times \text{anti-scalant} \\ \text{dose rate} + \text{chlorine} \times \text{chlorine dose rate} \end{array} \right) \quad (29)$$

Hence, the relation for thermo-economic distillate cost would become as follows:

$$C_d = \frac{C_{fi} E_{fi} + C_{steam-med} \Delta Ex_{steam} + Z_{med}^{IC\&OM}}{Ex_d} \quad (30)$$

4. Design operating conditions

4.1. MATS concept (SSRC)

As indicated earlier, this technique (SSRC) consists of two pumps for circulation and pressure drop, solar collector field (PTC), BHX, turbine expander unit, and MED with two effects. The first MED effect would be operated as a condenser unit for the steam Rankine cycle. Table 3 shows and summarizes the design points of this technique. Fig. 2 shows the flow diagram of this concept. Appendix-A shows the thermo-physical properties of the molten salt heat transfer medium. For the domination of long operation along the year with a daylight of 24 h, the

Table 3
Design and input data points for MATS concept configuration (SSRC)

Parameter	Design point
Environment	
G_b , W/m ²	500
Ambient temperature T_{amb} , °C	25
Inlet seawater temperature T_{sea} , °C	20
Solar PTC	
Outlet PTC temperature T_{co} , °C	550
Loop mass flow rate, kg/s	1
Collector width, m	5.9
Length, m	100
Glass envelope diameter, m	0.11
Inner tube diameter, m	0.0655
Working fluid	Heat transfer molten salt (HTS)
Boiler heat exchanger (BHX)-storage	
BHX effectiveness, %	80
BHX inner/outer tube diameter, m	0.0127/0.0129
Storage tank pump efficiency, %	75
Super heat temperature, °C	450
Hot side/cold side	Molten salt (HTS)/water steam
Steam turbine	
Working fluid	Water steam
Turbine and generator efficiency, %	85, 95
MED-PF	
Working fluid (hot side/cold side)	Water steam/Seawater
Last effect temperature T_{bn} , °C	60
TST to the MED, °C	71–75
Feed salinity, ppm	35,000
Brine blow down salinity, ppm	55,000
Seawater end condenser effectiveness, %	80
No. of effects	2
Productivity, m ³ /d	250

solar radiation would be estimated and fixed at 500 W/m² (21.4 MJ/m² = 503.7 W/m²) [11,22].

4.2. SORC concept

This configuration differs from the MATS concept according to the working fluid that been used. Fig. 3. shows the flow diagram of SORC configuration. Table 4 illustrates the design input data points for the ORC technique. The configuration consists of solar PTC with Therminol-VP1 heat transfer oil (HTO), BHX unit for thermal power transfer (intermediate unit), turbine unit (power generation), recuperator for regeneration, MED for freshwater, and the pumping system. Therminol-VP1 HTO is used through

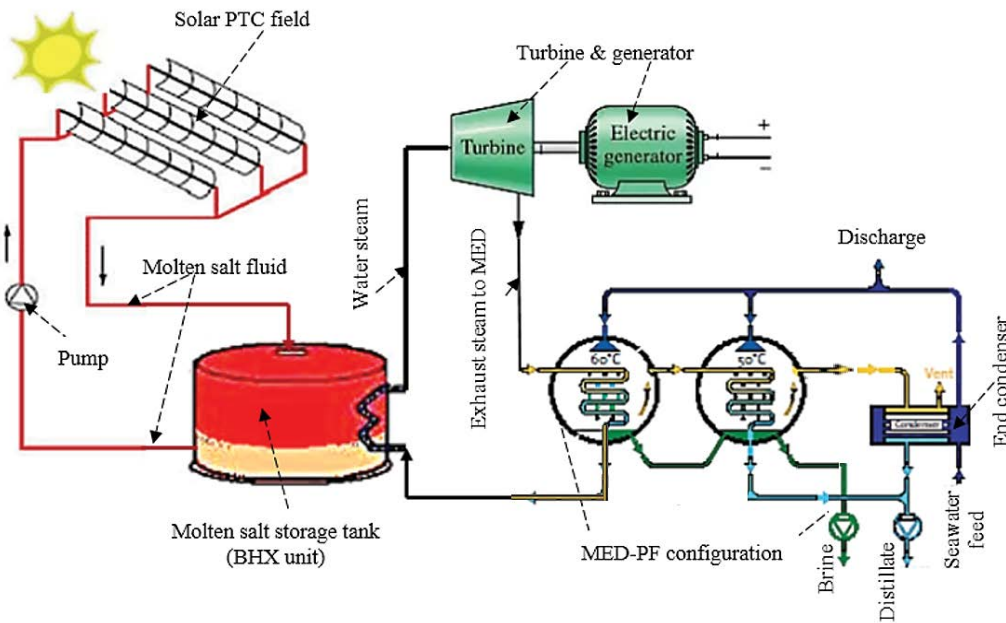


Fig. 2. Schematic flow diagram of SSRC (MATS reference concept): solar PTC, molten salt storage tank, turbine unit, MED-PF with air-cooled end condenser unit and pumps.

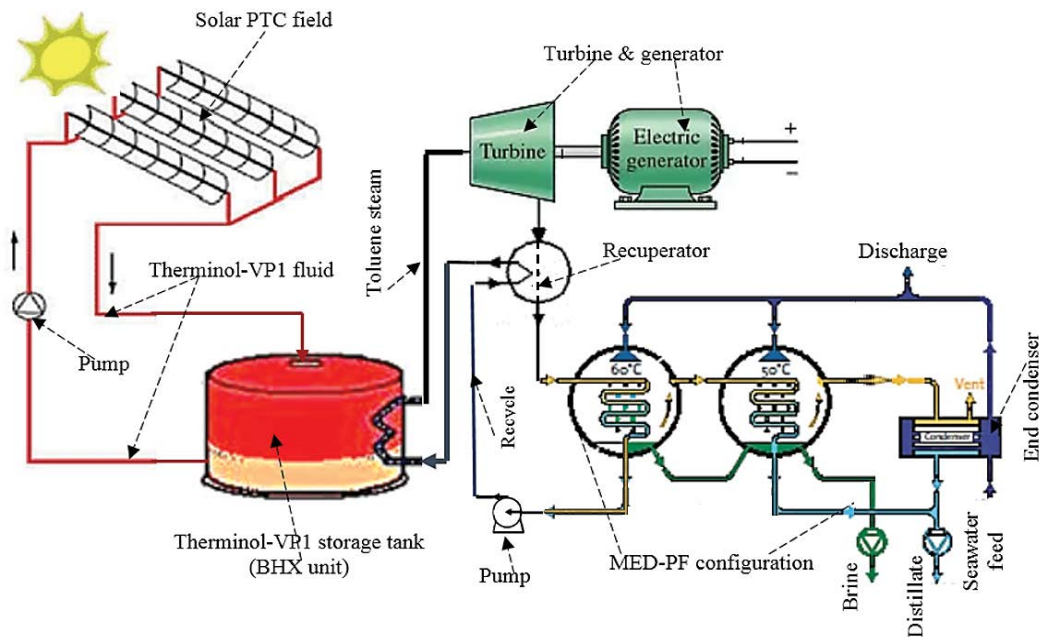


Fig. 3. Schematic flow diagram of SORC proposed configuration: solar PTC, BHX unit with therminol-VP1 heat transfer oil, turbine unit, recuperator, pumps, and MED-PF with end condenser.

the solar thermal cycle [31]. Therminol-VP1 is quite suitable for PTC because its top temperature can be reached at 450°C–500°C without any severe stresses on the absorber tube of the PTC combined with a maximum pressure no more than 15 bar. Another advantage of using HTO is that it does not need any external source of heat to prevent freezing as happening in molten salt operation. Figs. 4c and d show the Therminol-VP1 behavior regarding pressure and enthalpy vs. temperature vs. molten salt working fluid.

Although molten salt can be operated with minimum pressure rates, it needs a reactor or fed heater in order to keep its lower temperature above 200°C leading to extra costs by adding more heat at the input stage to the PTC field. It may cause some problems under winter operating conditions. Appendix-B addresses the thermo-physical properties of the Therminol-VP1 HTO. Toluene is used though the Rankine cycle to generate sufficient power. The selection of Toluene was performed and studied before by Nafey and Sharaf [36].

Table 4
Design points considered for solar ORC concept configuration (SORC)

Parameter	Design point
Environment	
G_{tr} , W/m ²	500
Ambient temperature T_{amb} , °C	25
Inlet seawater temperature T_{sea} , °C	20
Solar PTC	
Outlet PTC temperature T_{co} , °C	350
Loop mass flow rate, kg/s	1
Collector width, m	5.9
Length, m	100
Glass envelope diameter, m	0.11
Inner tube diameter, m	0.0655
Working fluid	Heat transfer oil (HTO)
Pump	
Working fluid	HTO
Efficiency, %	75
Boiler heat exchanger (BHX)-storage	
BHX effectiveness, %	80
BHX inner/outer tube diameter, m	0.0127/0.0129
Tank pump efficiency, %	75
Dry steam temperature, °C	160
Hot side/cold side	HTO/Toluene
Steam turbine	
Working fluid	Toluene
Efficiency, %	85
Generator efficiency, %	95
Recuperator	
Effectiveness, %	80
Inlet temperature, °C	Depending on turbine outlet
Hot side/cold side	Toluene/Toluene
MED-PF	
Working fluid (hot side/cold side)	Toluene/Seawater
Last effect temperature T_{bn} , °C	60
TST to the MED, °C	71–75
Feed salinity, ppm	35,000
Brine blow down salinity, ppm	55,000
Seawater end condenser effectiveness, %	80
No. of effects	2
Productivity, m ³ /d	250

Figs. 4a and b show the positive slope behavior of the toluene regarding to temperature and enthalpy while comparing against water. It is pinpointed from the figure that using recuperator is particularly important because of the outlet

turbine condition is still in super heat region. Appendix-C addresses the thermo-physical properties of the toluene working fluid. The selection of toluene depends on many criteria the most important of which is the maximum temperature of the cycle. The following criteria are achieved by toluene working fluid [35,36]:

- High molecular weight to reduce the turbine nozzle velocity.
- Reasonable pressure corresponding to boiling temperature of the fluid (high pressure requires careful sealing to avoid leakage). Dry expansion, that is, positive slope of the vapor saturation curve on T - S diagram, to assure that all expansion states in the turbine exist on the superheat region (Fig. 4). Regeneration can increase the inlet exergy stream or decreasing the total exergy destruction rate for the whole cycle. A critical temperature well above the maximum operating temperature of the cycle and reasonable pressure at condensing temperature (usually about 30°C–50°C).

4.3. Modeling and simulation

The proposed scenarios in this work require an iterative program to work out the complicated streams (recycle and backward streams). Hence, the authors used REDS software library [23,24,34] to perform the projected scenarios. Models are constructed according to the proposed configurations (SSRC and SORC). The models are built according to design calculation method. The system border streams (outlet temperature, ambient temperature, inlet cooling water temperature, etc.) are assigned by the user than the entire design data (area, length, volume, mass flow rate, etc.) will then be calculated. The simulation time was set at “inf” while changing the design points to go through a dynamic model simulation. The user would assign the amount of needed freshwater net production from the desalination plant then all possible or required design data for all the system units would be calculated in sequence. Specifying the system productivity would calculate the required thermal load (in case of MED-PF). Besides, the required design limits and performance calculations would be pass out instantly.

For thermal configuration, the thermal load would calculate the mass flow rate and the considered physical properties. The argument functions would call the data stored in the lookup tables and correlations that been embedded inside the code. Saturated liquid and vapor phases of pressure, temperature, enthalpy, specific volume, and specific entropy are stored behind the modeled blocks.

Fig. 5 shows the example of recuperator unit based on Matlab/Simulink environment. It is pinpointed from Fig. 5 that the interface block is containing the code block which is represented by inputs and outputs streams. As shown in the Fig. 5, the effectiveness should be assigned because of the use of design technique of modeling. The model block is exhibited to treat the input parameters such as temperatures, and flow rates based on function code to represent the block outputs such as temperatures, area, cost streams, exergy streams, and energy.

Generally, the optimization process has been done to bring down costs and techno-economic solutions. Desalination

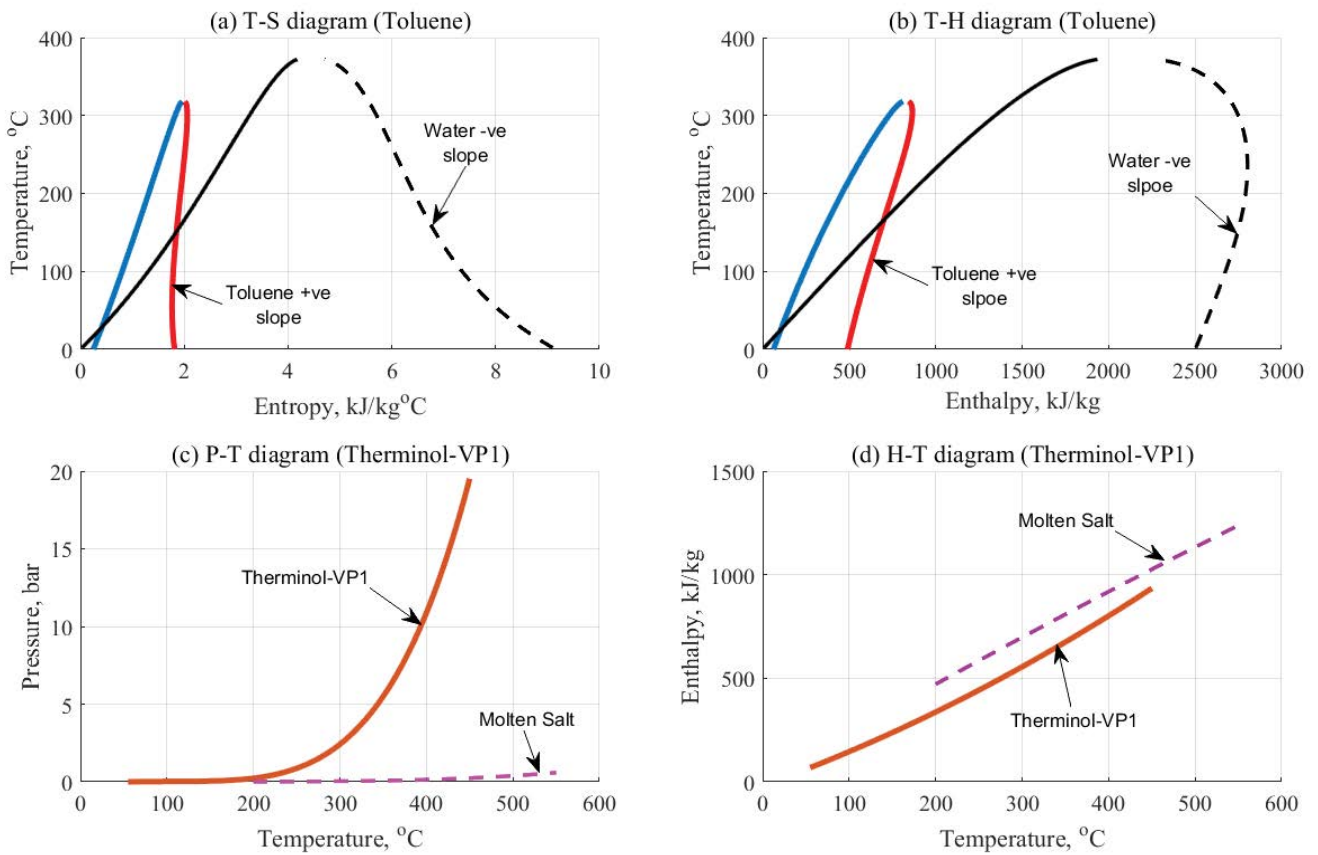


Fig. 4. (a) Toluene positive slope behavior regarding to $T-S$, (b) $T-H$, (c) therminol-VP1 based on $P-T$, and (d) $H-T$ diagrams.

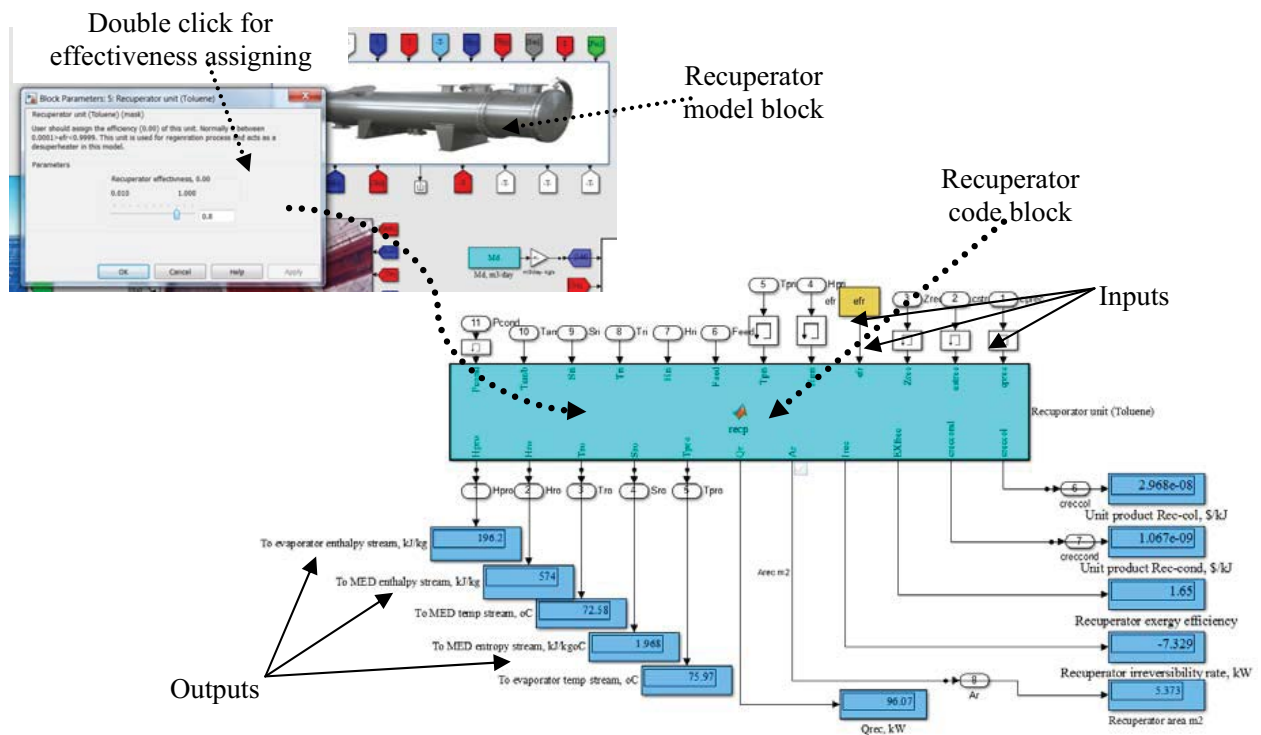


Fig. 5. Recuperator model browser as an example of SDS-REDS MatLab/Simulink toolbox.

plants were optimized to lower the thermal loads on the first effect for MED. In this work, a power generation scenario has been considered. In that scenario, the investor will be caring about the power developed from the plant regardless of the other parameters (area, cost, and productivity). The assumption based on this scenario is to generate 100 MWe. Therefore, the results would give us a clear decision about the possibilities of generation 100 MWe of electric power.

5. Results and discussions

In this section, techno-economic evaluation of two (SSRC and SORC) different CSP combined with MED are performed and presented in this section. SSRC is represented as MATS reference concept. However, SORC is represented as the proposed solar organic (Toluene) Rankine cycle. Meanwhile, optimization of operating conditions and design limits are considered for each configuration (SSRC and SORC).

5.1. Results of SSRC technique

As indicated earlier, SSRC using molten salt is constructed for just two MED-PF effects. The target was to desalinate 250 m³/d and to produce about 1 MWe. The brine blow down temperature was fixed at 60°C, which is considered relatively high. This temperature was set by the designer to decrease the temperature drop between the MED effects. For two effects, the temperature drop is around 5°C. Otherwise, increasing the number of MED effects should be considered rather than working on high degree of blow down temperature. The steam condensate temperature was fixed at 70°C. The effect of these two parameters was found to be massive especially the blow down temperature while operating at two MED effects. Fig. 6 shows the effect of these two parameters (blow down and steam condensate temperatures) is measured on some important parameters such as PTC area, the developed power, exergy destruction rate, thermo-economic product cost, and total hourly costs. It is

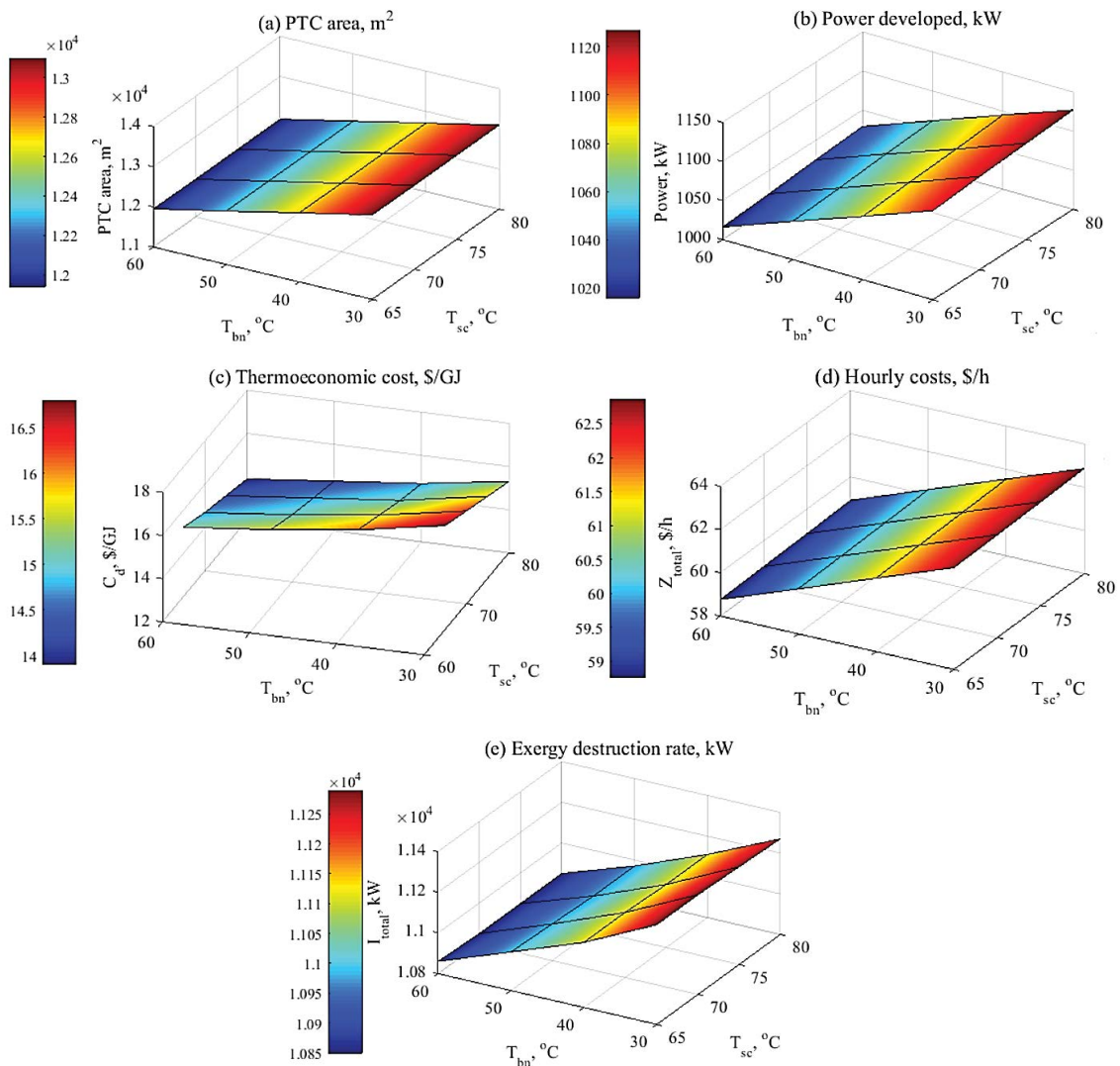


Fig. 6. Data results for SSRC based on brine blow down and steam condensate temperatures: (a) PTC area, m², (b) power developed, kW, (c) thermo-economic product cost, \$/GJ, (d) total plant hourly costs, \$/h, and (e) exergy destruction rate, kW.

obvious from Fig. 6a that increasing these two parameters will cause a significant change in the PTC area. However, the massive effect has found caused by the blow down temperature (T_{bn}). Increasing the T_{bn} will decrease the PTC area by 8.5%–9% which is considered huge especially while comparing at large amounts of system productivity. For T_{sc} , the change was not exceeding over 0.8%. The remarkable conditions have found at T_{bn} equal to the range of 50°C–60°C and T_{sc} equal to 70°C. That is because of the decreasing of temperature drop between MED effects. T_{bn} can be reduced in case of increasing the number of MED effects. Fig. 6b shows the effect these two parameters on the developed power by the turbine unit. The same behavior was found regarding to the T_{bn} effect. The percentage of change between $T_{bn} = 30^\circ\text{C}$ and 60°C was 9.8%–10% increasing in the developed power by the turbine unit. Therefore, it has found that to generate more power, it is urgent to decrease the T_{bn} temperature, hence, increasing the PTC area at the same time. It is dependent on the investor and/or the designer to decide between power and area. For thermo-economic product cost (Fig. 6c), \$/GJ, the change was remarkable by achieving a percentage of change reached to 17.8%–18%. However, the best value of T_{bn} was found between 45°C and 50°C depending on number of MED effects. The thermo-economic parameter is particularly important because it reflect the combination between cost and exergy. At the same time, the exergy is also reflecting the maximum available work (gain) that be extracted from any system putting in considerations the entropy generation minimization. Fig. 6d shows the effect of T_{bn} and T_{sc} on the total hourly costs, \$/h. The percentage of change was about 5.9%–6% while increasing the T_{bn} up to 60°C. This the direct reflection to the decreasing of the PTC area in Fig. 6a. Therefore, a value between 50°C and 60°C is quite interesting to decrease the PTC area and total costs just for low numbers of MED effect or units. Fig. 6e shows the change of total exergy destruction rate in kW. The percentage of change between 30°C and 60°C was about 3.6%–4% decreasing. That is mean, the operation at high levels of T_{bn} at low numbers of MED effects is quite interesting. Therefore, it is quite interesting to utilize the values of 45°C–50°C for T_{bn} and 70°C for T_{sc} temperature. Increasing the temperature drop between effects would increase the performance of the MED by 75% (2 vs. 8 MED effects). Table 5 shows the results of SSRC technique based on the new characteristics addressed for 250 m³/d.

It is clear from this configuration (SSRC) results that there are some defects, which have some negative effects on the performance of the MED and the total plant side. There are some recommendations to overcome that defect

Table 5
Data results for solar SRC concept configuration (SSRC)

Parameters	
PTC	
T_{cr} °C	167.4
T_{co} °C	550
M_{col} kg/s	5.128
A_{col} m ²	1.2223e-4

No. of loops	6
I_{col} kW	3,472
$C_{pstg-col}$ \$/kJ	4.731e-5
$C_{col-bhx}$ \$/kJ	1.307e-5
Z_{col} \$/h	28.96
BHX unit	
T_{msi} °C	550
T_{mso} °C	167.4
T_{ev} °C	71.76
T_{evs} °C	265
V_{bhx} m ³	93.16
Pump power, kW	0.6078
Thermal load, kW	4,317
A_{bhx} m ²	8.934
I_{bhx} kW	286.8
$C_{bhx-tur}$ \$/kJ	1.527e-5
$C_{pstg-col}$ \$/kJ	4.731e-5
C_{p-bhx} \$/kJ	7.753e-5
Z_{bhx} \$/h	0.08
Turbine unit	
T_{to} °C	71.65
Power, kW	1,040.11
Dryness fraction, %	96.96
M_{sv} kg/s	1.436
I_{tur} kW	813.1
C_{ur} \$/kJ	3.232e-5
$C_{tur-med}$ \$/kJ	1.527e-5
Z_{tur} \$/h	19.13
MED-PF (two effects)	
T_s °C	71.65
T_p °C	43.5
T_d °C	25.88
T_{bi}/T_{bn} °C	61.14/50
GR	1.87
A_{med} m ²	2.6438e-2
A_{econd} m ²	124.1
M_{fr} kg/s	34.88
M_p kg/s	7.957
M_{cv} kg/s	26.93
M_s kg/s	1.436
I_{med} kW	1.664e-4
C_{med-p} \$/kJ	1.527e-5
C_d \$/GJ	18.08
Z_{med} \$/h	654
Pump unit	
T_{po} °C	71.76
Power/ I_{pump} kW	9.975/9.12
C_{p-bhx} \$/kJ	7.753e-5
Z_p \$/h	0.2268

Working fluids = MS and water steam, $T_{bn} = 50^\circ\text{C}$, $T_{sc} = 70^\circ\text{C}$, $T_{drysat} = 265^\circ\text{C}$, $T_{sup} = 450^\circ\text{C}$, $T_{amb} = 25^\circ\text{C}$, and $M_d = 250 \text{ m}^3/\text{d}$.

such as decreasing the brine blow down temperature combined with increasing the number of the MED effects. Although the T_{bn} is around 60°C, but it is not favorable at all. It is recommended to increase the number of MED effects rather than increasing the T_{bn} temperature. Reducing the top steam temperature is also in study combined with increasing the number of MED effects. Molten salt operation needs more thermal energy and would increase the inlet turbine condition, which is not fit well for the MED operation (relatively low-temperature operation while comparing against MSF).

5.2. Results of SORC technique

This technique is differ from the previous one according to the following criteria: (i) the working fluids used, (ii) toluene operating conditions on the T–S diagram, (iii) turbine inlet conditions, and (iv) the top solar PTC temperature, and (v) the regeneration process via recuperator unit. However, both techniques are considered the same according to the system modules and units that have been applied. Fig. 7 shows the SORC operating conditions on the T–S diagram. Utilizing the organic Rankine concept instead of steam would decrease the degree of risks of using water steam and molten salt operating conditions. Furthermore, the outlet turbine condition will be remaining in super heat region (Fig. 7) allowing by this to add the recuperator unit for regeneration stage before the solar field. That would decrease the load on the solar PTC, that is, decreasing the total solar field area. Table 6 shows the data results obtained for this technique. It is clear from Table 6 that SORC technique gives a remarkable result based on two MED effects.

The dry saturated temperature is fixed at 160°C to adjust the inlet steam temperature to the first MED effect at 71°C–72°C. The solar field area has decreased by 450 m² while comparing against the first technique (SSRC). This result has considered a promising result because it will effect on the total thermo-economic product cost parameter. The same results has noticed on the MED heat transfer area. The total heat transfer area is recorded as 255 m² against 265 m² for the first technique (SSRC). The power developed from the first technique was about 1,000 kW against 920 kW for the SORC which both are considered the same in power range. For thermo-economic product cost parameter (C_d \$/GJ), SORC gives superior results at the same plant productivity. As indicated earlier, C_d is a direct reflection to the cost and the exergy streams through the system units. The C_d for this technique is reduced by 28%–30% while comparing against the SSRC technique. It gives about 14 \$/GJ against 19–20 \$/GJ which is considered impressive result putting in consideration cost and exergy. Fig. 8 shows the thermo-economic cost streams for SORC configuration. It has been shown from Fig. 8 that the cost of power stream gave the highest value among the other streams followed by pumping streams (C_w \$/GJ = 2.2, $C_{pstg-colv}$ \$/GJ = 1.7). That effect has happened because of that the power cost is depending on high values of hourly cost parameter and inlet exergy stream related to turbine and pumps units. Although MED gives the highest hourly cost value (185 \$/h), however, the inlet exergy stream or the gain from distillate stream is high enough to reduce the cost streams to or from the MED process. The same behavior is noticed on the hourly cost parameter for the solar field (Z_{colv} \$/h). SORC technique gives a value of 11 \$/h against 28–30 \$/h for SSRC.

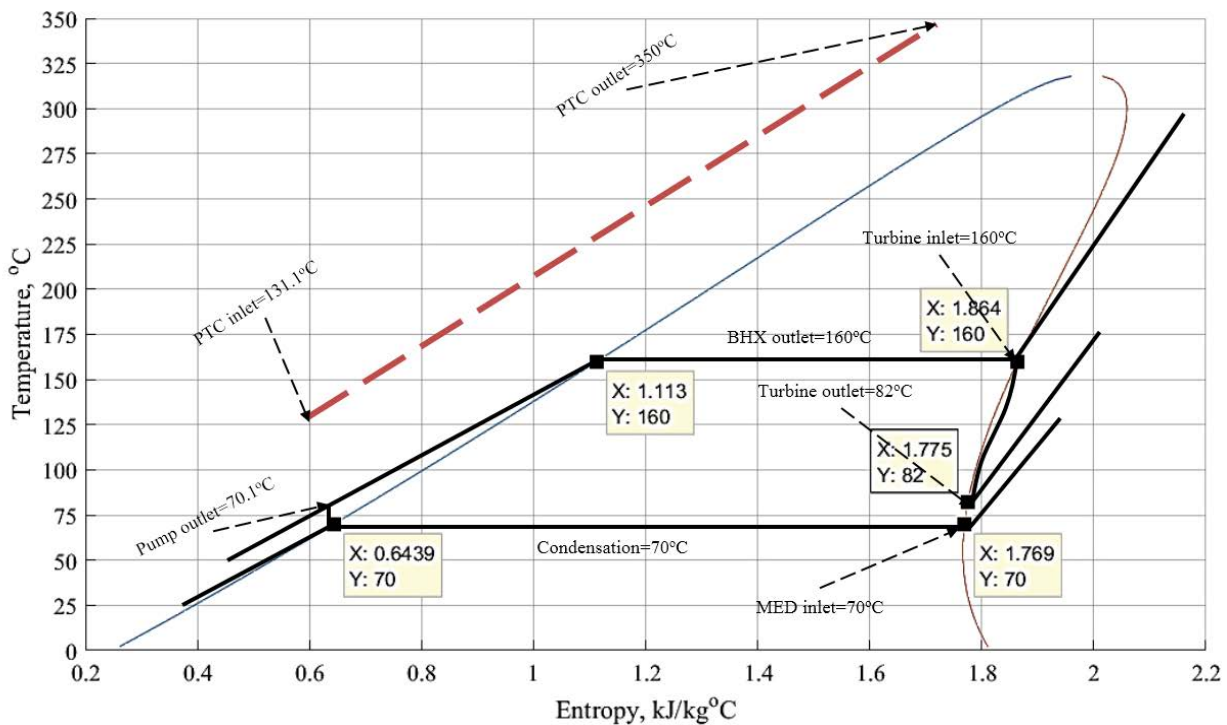


Fig. 7. SORC operating conditions on the T–S diagram.

Table 6
Data results based on the N_{eff} for solar ORC concept configuration (SORC)

Parameters	$N_{\text{eff}} = 2, T_{\text{bn}} = 50^\circ\text{C}, T_{\text{sc}} = 70^\circ\text{C},$ $T_{\text{drysat}} = 160^\circ\text{C}, T_{\text{amb}} = 25^\circ\text{C},$ $M_d = 250 \text{ m}^3/\text{d}$
PTC	
$T_{\text{cfr}} \text{ }^\circ\text{C}$	131.1
$T_{\text{cof}} \text{ }^\circ\text{C}$	350
$M_{\text{colf}} \text{ kg/s}$	9
$A_{\text{colf}} \text{ m}^2$	1.18e-4
No. of loops	9
$I_{\text{colf}} \text{ kW}$	3,557
$C_{\text{pstg-colf}} \text{ } \$/\text{kJ}$	1.761e-6
$C_{\text{col-bhx}} \text{ } \$/\text{kJ}$	1.683e-6
$Z_{\text{colf}} \text{ } \$/\text{h}$	11.66
BHX unit	
$T_{\text{evif}} \text{ }^\circ\text{C}$	75.97
$T_{\text{evof}} \text{ }^\circ\text{C}$	160
$A_{\text{bhxf}} \text{ m}^2$	11.34
$I_{\text{bhxf}} \text{ kW}$	721.8
$C_{\text{bhx-turf}} \text{ } \$/\text{kJ}$	1.125e-9
$Z_{\text{bhxf}} \text{ } \$/\text{h}$	0.009–0.01
Turbine unit	
$T_{\text{tor}} \text{ }^\circ\text{C}$	82.33
Power, kW	916.87–920
$M_{\text{orc}} \text{ kg/s}$	8.6
$I_{\text{turf}} \text{ kW}$	369
$C_{\text{tr}} \text{ } \$/\text{kJ}$	3.089e-6
$C_{\text{tur-med}} \text{ } \$/\text{kJ}$	1.125e-9
$Z_{\text{turf}} \text{ } \$/\text{h}$	7.25
Recuperator unit	
$T_{\text{rof}} \text{ }^\circ\text{C}$	72.58
Area, m^2	5.54
$C_{\text{rec-col}} \text{ } \$/\text{kJ}$	2.8e-8
$C_{\text{rec-cond}} \text{ } \$/\text{kJ}$	1.123e-9
$Z_{\text{rec}} \text{ } \$/\text{h}$	0.00541
MED-PF	
$T_{\text{sf}} \text{ }^\circ\text{C}$	72.58
$T_{\text{sf}}, T_{\text{dt}} \text{ }^\circ\text{C}$	43.5, 25.88
$T_{\text{bl}}/T_{\text{bn}} \text{ }^\circ\text{C}$	70.3/50
GR	1.88
$A_{\text{medt}} \text{ m}^2$	253.45–255
$M_{\text{rf}}, M_{\text{cw}}, M_{\text{sf}} \text{ kg/s}$	34.87
$M_{\text{f}}, \text{ kg/s}$	7.957, 26.92–27, 8.611
$I_{\text{medt}} \text{ kW}$	1.7e-4
$C_{\text{med-pf}} \text{ } \$/\text{kJ}$	1.125e-9
$C_{\text{dt}} \text{ } \$/\text{GJ}$	14.73 < SSRC
$Z_{\text{medt}} \text{ } \$/\text{h}$	186.87
Pump unit	
$T_{\text{pof}} \text{ }^\circ\text{C}$	70.14
Power/ I_{pump} , kW	4.42/1.88
$Z_{\text{pf}} \text{ } \$/\text{h}$	0.1

Fig. 9 shows that MED gives the highest values of the hourly costs followed by solar field. Therefore, it is quite interest to reduce the DCCs for MED and PTC. It is clear from this technique's result that organic Rankine operation have many advantages against the SSRC. The hourly costs are decreased against the molten salt operation because of low operating conditions of the PTC field. The MED hourly costs are considered very low while comparing against the molten salt steam operation (186 vs. 654 \$/h). Positive slope of the toluene working fluid gives it an advantage against the water steam operation with negative slope on the T - S diagram. Meanwhile, the regeneration through the recuperator unit helps to regain some of the heat input to the PTC field leading to decreasing the total area of the solar field. There is no need to operate the solar field over 350°C – 400°C to avoid the thermal stresses and losses to the ambient.

5.3. Power generation scenario comparison

In this scenario, the investor is caring about the power developed from the plant regardless of the other parameters (area, cost, productivity). The assumption based on this scenario is to generate 100 MWe. Therefore, the results would give us a clear decision about the possibilities of generation 100 MWe of electric power. The number of effects is set as eight effects to reduce the total plant costs. Fig. 10 shows a schematic diagram of the eight MED effects that been considered in this scenario. The steam from SORC or SSRC would be responsible about the thermal power generation of the first effect of the MED. Steam cycle will be considered a separate cycle from the MED by considering the first effect to be treated as a condenser unit for the power cycle.

Table 7 shows clearly the differences between these two concepts based on power development. As expected, increasing the required power from the turbine unit would increase all design aspects as a normal load overall on the plant. However, there is an advantage to the SORC because of the water production rate is massively increased by 11.7% against the SSRC concept. Sure, all mass flow rates are increased; however, productivity as an exergy outlet (positive gain from the system) is also increased.

Moreover, the total cycle steam flow rate is considered massive regarding the SORC concept by an increasing percentage of 85.3%. Regarding the area, the general deviation was varying between 7% and 11%. It has noticed that SORC has conceded more areas in general because of the large amounts of mass flow rates through the units. For example, the SORC PTC area was exceeding by 7.68%. While the MED area for the same technique was exceeding by 7.15% for the same reason.

Meanwhile, the same effect has noticed regarding the end condenser unit. Regarding the power, the SORC concept has the lead in total exergy inlet by a percentage of 7.68%, which is considered a valuable result for the effect on the thermo-economic parameter. SSRC destruction rate was less by 11.35% giving an advantage to this concept. This is because of the operation of a relatively low mass flow rate compared to the SORC concept.

Pumping power results are reflected in the mass flow rates increasing. SSRC concept is noticed less in pumping power by 17%. Regarding cost terms, the SORC concept has remarkably found attractive. This is particularly important

to the investors according to the lower cost achievements by the SORC concept. The hourly costs for the SORC were found less by 36% with total water rice 12.24% lower than the SSRC concept.

That result is so promising and gives an advantage to the SORC concept. Moreover, the thermo-economic product cost parameter ($C_{p,}$ \$/GJ) is found remarkable for the SORC concept by 91% of decreasing. Therefore, it is noticeably clear to the investor that the SORC concept is dominantly based on the terms of power scenario in case of 100 MWe operation. Fig. 11 shows the variations of exergy destruction rate, productivity, hourly costs, and PTC area against the variation of power generation.

For all the mentioned parameters in Fig. 11, increasing the power generation would increase the behavior of these parameters. For Figs. 11a, b, and d, there is a slight difference between both configurations. However, the productivity gain from SORC configuration is slightly high by 11%. Fig. 11a shows the difference between SORC and SSRC regarding to the specific exergy destruction rate ($SED = \text{exergy destruction/power developed}$). It is indicated from Fig. 11a that SORC gives an attractive lower result against the SSRC. Both behaviors are in decreasing mode while increasing the power developed from the system. Fig. 11c shows that the thermo-economic product cost, \$/GJ

for SSRC is much greater than the SORC. SORC gives lower thermo-economic product cost values concerning power generation regardless of the exergy destruction rate. This behavior is a huge advantage to the SORC configuration because the investor will be much care about the cost combining with the exergy rates. Fig. 11c shows that the thermo-economic product cost was in the range of 0.12–3.6 \$/GJ which is considered extremely attractive against the SSRC configuration. Fig. 12 shows the effect of power generation from the proposed systems on the levelized power cost parameter (LPC, \$/kWh) in case of competing against the ranges between 100 and 700 MWe. SORC shows an attractive result on Fig. 12 while comparing against SSRC (0.025 vs. 0.04 \$/kWh and vs. 0.07 \$/kWh for CSP + PV [41]). For mainly basic cases, MATS concept regarding to steam or organic can be adopted if the solar tower not considered in this relation as existed in NOOR ENERGY 1 solar power plant [41].

5.4. Real time simulation results

It is particularly important to drive out the results of the proposed configurations (SSRC and/or SORC) based on real-time simulation with respect to a time span of 9 h as an example. In this section, it is assumed to run out the simulation results based on the following operating conditions:

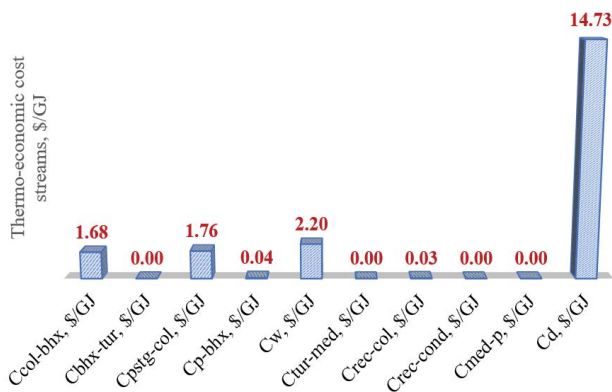


Fig. 8. Thermo-economic cost streams for SORC configuration.

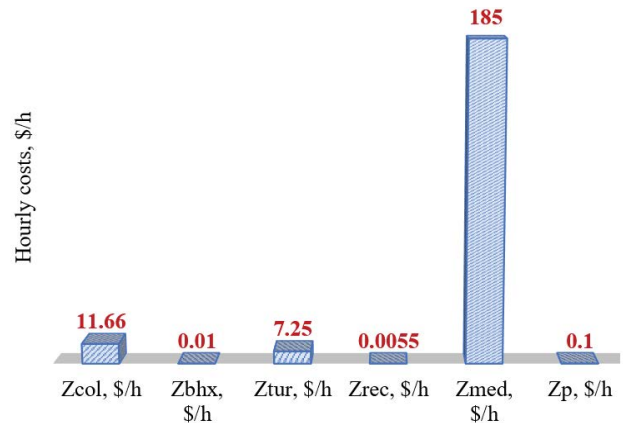


Fig. 9. SORC hourly cost parameter results.

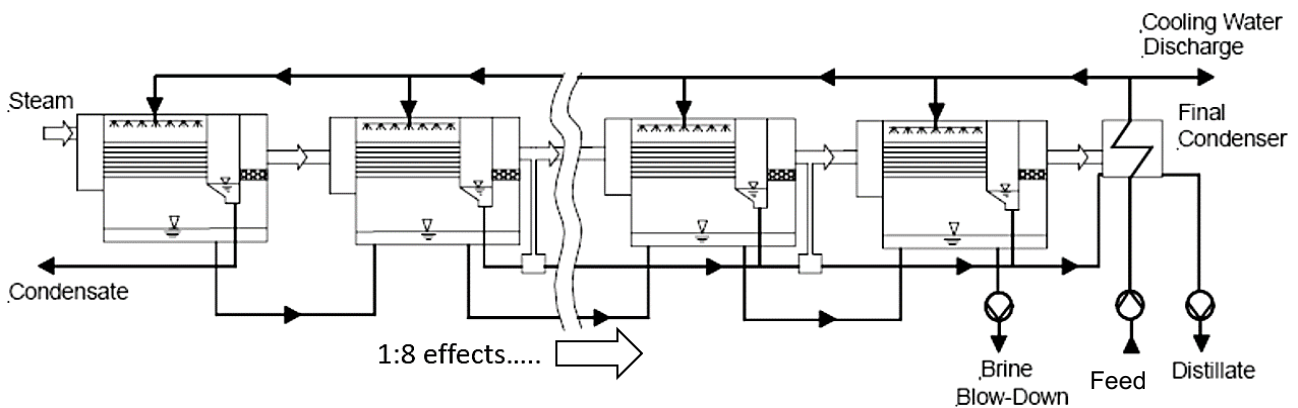


Fig. 10. Schematic diagram of the eight MED effects.

Table 7
Data results comparison for SSRC and SORC based on power scenario

Parameters	Power = 100 MWe, $N_{eff} = 8$		
	SSRC	SORC	Deviation to SORC, %
M_v , kg/s	138.2	939.8	+85.3%
M_{col} , kg/s	493.4	984.5	+49.88%
M_{fr} , kg/s	3,272	3,706	+11.71%
M_{cv} , kg/s	273.3	308.2	+11.32%
M_{dr} , m ³ /d	94,200	106,750	+11.75%
M_b , kg/s	1,907.99	2,162.18	+11.75%
GOR	7.87	7.88	-0.53%
PTC area, m ²	1.1761e-6	1.274e-6	+7.68%
MED area, m ²	4.9789e-5	5.36244e-5	+7.152%
End condenser area, m ²	1.164e-4	1.318e-4	+11.68%
Turbine power, kW	100,000	100,000	0
Total pumping power, kW	9,815	1.181e-4	+16.9%
I_{total} , kW	2.81e-6	3.17e-6	+11.35%
Ex_{in} , kW	5.491e-5	5.948e-5	+7.68%
Z_{total} , \$/h	4,215	2,699	-36%
TWP, \$/m ³	1.1	0.9653	-12.24%
Power cost, \$/kWh	0.042	0.027	-55%
C_d , \$/GJ	3.75	0.3403	-91%

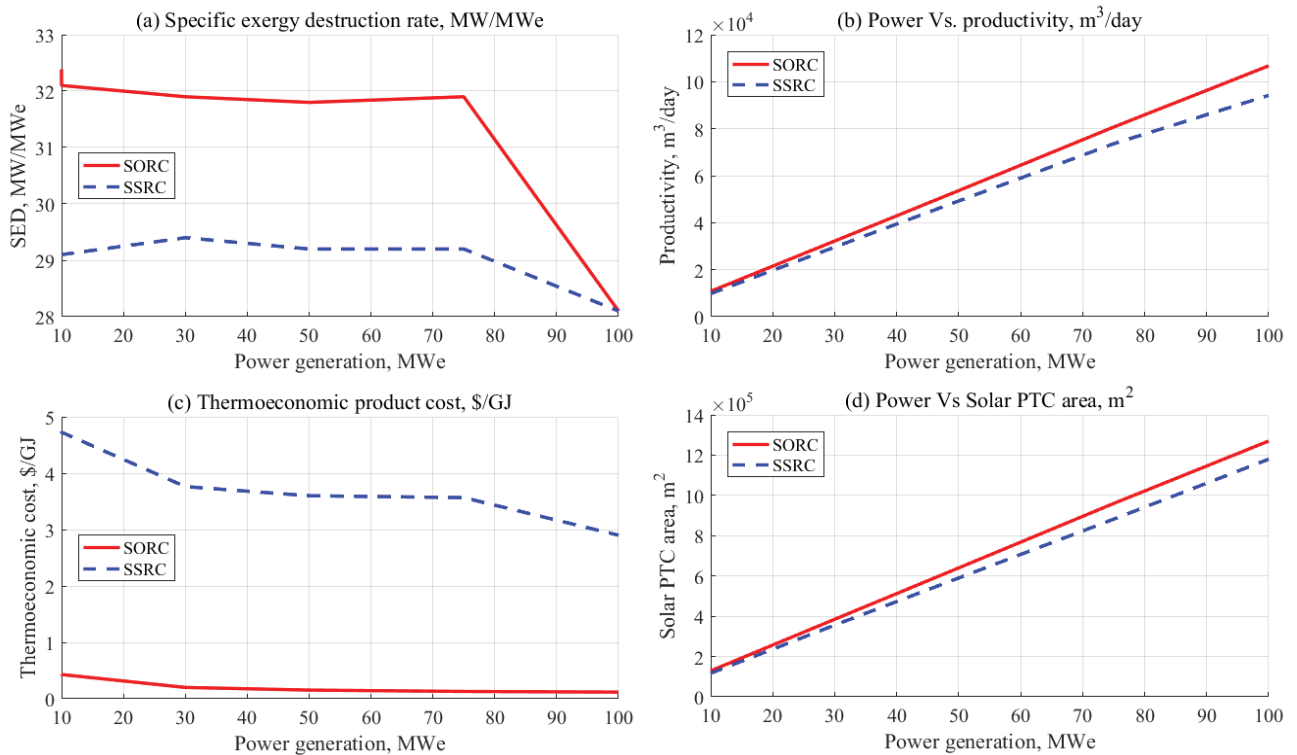


Fig. 11. Data results based on the power scenario for both configurations: (a) SED, MW/MWe, (b) plant productivity, m³/d, (c) thermo-economic product cost, \$/GJ, and (d) solar PTC area, m².

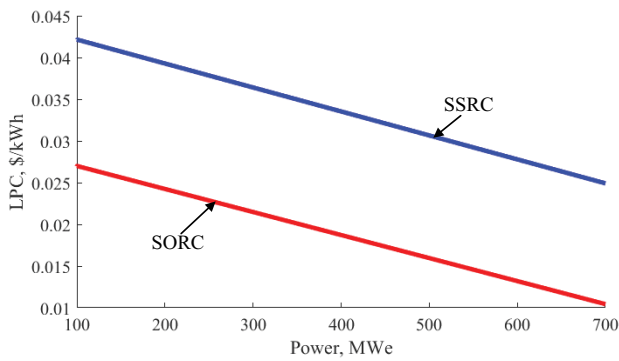


Fig. 12. Effect of power generation of both systems on the levelized power cost parameter, \$/kWh within the range of 100–700 MWe.

- Simulation time span has been fixed at 9 h from 8:00 a.m. to 4:00 p.m. The simulator configured each 1 s as 1 h. The effect of changing the instant solar radiation (W/m²) on the hourly costs of both configurations (SSRC and SORC) is performed. A typical Julian day in spring (day number = 60) was taken as a test day for this simulation. The location is set as inside the City for Science and Technology (SRTA-City) in Borg El-Arab, Alexandria-Egypt (30.9336° N, 29.6956° E). Solar radiation model by REDS [23,24,34,42] has been used.
- The effect of changing the dry saturated temperature (inlet turbine condition) on both configurations is performed. For SSRC configuration, the temperature variation was ranged from 250°C up to 280°C. For SORC configuration, the temperature range was about 139°C up to 165°C. For seawater temperature, the temperature range was between 10°C and 28°C. The plant productivity is set at 5,000 m³/d with eight MED effects for both configurations.

Signal generator block is used to generate these four parameter as dynamic values with respect to time domain. The signal builder block allows to create interchangeable groups of piecewise linear signal sources and use them in a model. Data variables are assigned as signals (matrix) in the signal generator block (MatLab/SimuLink) as indicated in Table 8.

Fig. 13 shows the real time results based on simulation time span 9 h: (a) thermo-economic product cost, \$/GJ, (b) total hourly costs, \$/h, (c) net power developed, kW, and (d) specific power consumption (SPC), kWh/m³. Fig. 13a shows the variation according to an especially important parameter which is the thermo-economic unit product cost (C_{gr}), \$/GJ.

That parameter reflects the combination between exergy and cost analysis. It remarkably noticed on Fig. 13a that SSRC conceded larger values of the C_{gr} \$/GJ while comparing vs. the SORC. SORC gives values within the range of 3.6 and 0.1006 \$/GJ which is considered exceptionally low. It is also clear that increasing the dry saturation temperature would decrease the C_{gr} \$/GJ.

The same behavior was also noticed on Fig. 13b regarding to the total hourly costs, \$/h. SSRC was recorded higher against the SORC. SORC gave a range of 250 to 350–400 \$/h while the SSRC gave a range of 800–1,400 \$/h as a maximum value. It is recommended to increase the dry saturation temperature to reduce the total hourly cost and the C_{gr} \$/GJ. For net power generation (Fig. 13c), SSRC would achieve a slight advantage in power development however, such advantage would increase the total hourly costs, that is, the C_{gr} \$/GJ. The net power developed was in the range of 5,000–5,500 kW for the SSRC and from 4,000 up to 4,700 kW related to SORC. Fig. 13d shows the data results according to the SPC, kWh/m³. It is obvious on Fig. 13d that the SPC, kWh/m³ was in a remarkable range (1.6–1.75 kWh/m³) for both configurations.

Such values a quite normal for solar MED plants while comparing against MSF and/or RO configurations. However, SORC achieves a slightly advantage against the SSRC with the same regard. Both configurations were in increasing mode based on the increasing of the dry saturation temperature. Generally, it is quite recommended to use organic working fluids such as toluene instead of using water steam regarding to some reasons such as:

- Stability along the thermodynamic process.
- Reaching to high values of top cycle pressure without low grades of thermal stresses.
- Superheat region is available at the turbine exhaust, that is, increasing the recovery grades for the system.
- Relatively lower hourly cost and thermo-economic product cost while comparing against the SSRC.

6. Conclusion

In this work, thermo-economic evaluation and analysis of different solar desalination cycles are presented and investigated. Two different configurations are analyzed with aim of freshwater production and electric power generation. The first configuration is caring about SSRC (MATS project concept) using molten salt working fluid through the solar PTC field. Water steam is used through the power cycle. The first configuration was built inside the City for Science and Technology (SRTA-City) in Borg El-Arab,

Table 8
Input data example based on dynamic model run

Parameter	Value
Time span, hs	[8 9 10 11 12 13 14 15 16]
Solar radiation, W/m ²	[150.3 273.35 421.3 544.7 603.1 577.7 476.7 332.9 193.92]
Dry saturation temperature (SSRC), °C	[250 255 257 260 265 268 270 275 280]
Dry saturation temperature (SORC), °C	[139 142 145 150 155 157 160 162 165]

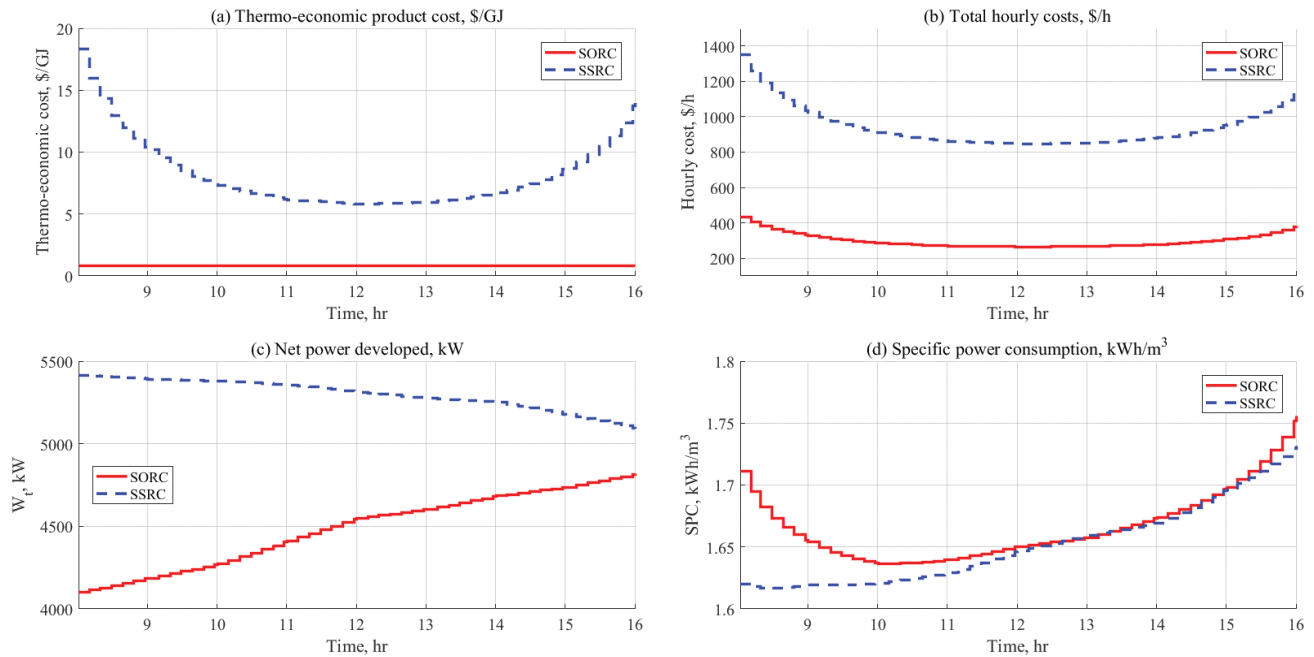


Fig. 13. Real time simulation results based on thermo-economic product cost, total hourly costs, net developed power, and specific power consumption.

Alexandria-Egypt. It is required by MATS configuration to desalinate and produce an amount of 250 m³/d of fresh-water and to generate about 1 MWe of power. The second configuration is a SORC with therminol-VP1 heat transfer oil through the solar PTC and toluene working fluid through the power cycle. Toluene is used in SORC because it shows a positive slope on the T - S , diagram. Hence, there is no need for super heat region; however, recuperator unit can be used for regeneration. For both configurations, the first MED effect is used as condenser unit. Both techniques are simulated and modeled by the aid of SDS-REDS software library. Based on the analysis performed in this work, the following conclusions can be draw:

- Different operating conditions such as inlet feed temperature, brine blow-down temperature, and dry saturated temperature are investigated for this evaluation.
 - Brine blow down temperature should be kept at relatively higher values (in case of use low numbers of MED effects) to decrease the temperature drop between the MED effects.
 - Increasing the number of stages up to eight effects would increase the gain ratio, hence, decreasing the total hourly costs.
 - Increasing the condensed steam temperature would increase the exergy destruction rates for both configurations.
- Decision about best-operating conditions is performed based on exergy, hourly costs, and thermo-economic product cost parameter.
- Power generation scenario which the investor is caring about the power generation (100 MWe) regardless the cost and the area. SORC gives lower thermo-economic product cost by 91% less than the SSRC configuration.

Moreover, it may give excess productivity by 11% than the SSRC.

- Dynamic modeling case studies are presented based on the dynamic changes of some operating conditions such as solar radiation, brine blowdown temperature, inlet feed seawater temperature, and dry saturated steam temperature.

According to the simulation results, SORC configuration gives attractive results against the SSRC based on thermo-economic product cost (14 vs. 19 \$/GJ), total hourly costs (205 vs. 704.5 \$/h), power cost (0.027 vs. 0.042 \$/kWh) and water price (0.9 vs. 1.12 \$/m³). For a range over 100 MWe (CSP + PV cases) SORC showed an attractive result on while comparing against SSRC (0.025 vs. 0.04 \$/kWh and vs. 0.07 \$/kWh for CSP + PV). It is highly recommended to use SORC instead of SSRC according to the results revealed in this study. Hourly costs and thermo-economic product costs are highly favorable while using SORC. Meanwhile, the thermo-economic product cost of the SORC was in the range of 0.12–3.6 \$/GJ which is considered extremely attractive against the SSRC configuration (3–5 \$/GJ). Real simulation data results according to the SPC, kWh/m³ show that the SPC was in a remarkable range (1.6–1.75 kWh/m³) for both configurations. Such values a quite normal for solar MED plants while comparing against MSF and/or RO configurations. Using molten salt as a heat transfer fluid needs more control on the inlet stream temperature to the solar PTC. The gain ratio is considered nearly the same for both configurations with little bit advantage to the organic cycle operation. For mainly basic cases, MATS concept (steam or organic) can be adopted without the existence of the concentrated solar tower as in NOOR ENERGY 1 power plant, UAE.

Symbols

A	—	Area, m ²
A_{col}	—	Solar field area, m ²
A_{BHX}	—	Boiler heat exchanger area, m ²
A_{cond}	—	Condenser area, m ²
A_f	—	Amortization factor, 1/y
ACC	—	Annualized capital cost, \$/y
B	—	Brine
BHX	—	Boiler heat exchanger unit
C	—	Cost, \$
CC	—	Capital costs, \$
C_p	—	Specific heat capacity at constant pressure, kJ/kg°C
$C_{\text{col-bhx}}$	—	Cost stream from solar collector to the BHX unit, \$/kJ
C_f	—	Feed cost stream, \$/kJ
$C_{\text{pstg-col}}$	—	Cost stream from storage tank pump to the solar collector, \$/kJ
$C_{\text{bhx-tur}}$	—	Cost stream from BHX unit to the turbine, \$/kJ
$C_{\text{p-bhx}}$	—	Cost stream from pump unit to the BHX unit, \$/kJ
C_w	—	Power cost stream, \$/kJ
$C_{\text{tur-med}}$	—	Cost stream from turbine unit to the MED, \$/kJ
C_d	—	Thermo-economic product cost, \$/GJ
D	—	Distillate
DCC	—	Direct capital cost, \$
Ex	—	Exergy rate, kW
Ex_{in}	—	Exergy in, kW
Ex_{out}	—	Exergy out, kW
F	—	Feed
G_b	—	Daily average direct irradiance, W/m ²
GR	—	Gain ratio = distillate mass flow rate/steam mass flow rate
h	—	Specific enthalpy, kJ/kg
HTO	—	Heat transfer oil
HTS	—	Heat transfer salt
I	—	Exergy destruction rate, kW
I_{total}	—	Total exergy destruction rate, kW
ICC	—	Investment capital costs, \$
IDCC	—	Indirect capital cost, \$
i	—	Interest, %
LF	—	Load factor
LT	—	Lifetime, year
M_d	—	Distillate mass flow rate, kg/s
M_s	—	Steam mass flow rate, kg/s
MED-PF	—	Multi-effect distillation parallel crossfeed arrangement
\dot{m}	—	Mass flow rate, kg/s
N_{pure}	—	Number of moles of pure water, gmol
N_{salt}	—	Number of moles of salt, gmol
N_{eff}	—	Number of effects
OC	—	Operating cost, \$
ORC	—	Organic Rankine cycle
S	—	Salinity ratio, kg/kg
s	—	Specific entropy, kJ/kg°C
SHC	—	Specific heating steam cost, \$/MkJ
SCC	—	Specific chemical cost, \$/m ³
SED	—	Specific exergy destruction rate, MW/MWe

SLC	—	Specific labor cost, \$/m ³
SPC	—	Specific power consumption, kWh/m ³
STPC	—	Specific thermal power consumption, kWh/m ³
SEC	—	Specific electrical cost, \$/kWh
T	—	Temperature, °C
TST	—	Top steam temperature, °C
T_{sun}	—	Sun temperature, 6,000 K
TCC	—	Total capital cost, \$
TWP	—	Total water price, \$/m ³
V	—	Volume, m ³
W_t	—	Turbine work, kW
W_p	—	Pump work, kW
$X_{w,s}$	—	Fraction of water and salt contents
$Z^{\text{IC\&OM}}$	—	Total investment and operating and maintenance cost, \$/h

Subscripts

amb	—	Ambient
av	—	Average
b	—	Brine
chm	—	Chemical
col	—	Collector
cond	—	Condenser
cw	—	Cooling water
d	—	Distillate product
f	—	Feed
i	—	In
MED	—	Multi-effect distillation
o	—	Out or reference
p	—	Pump
rec	—	Recuperator
s	—	Salt
stg	—	Storage
t	—	Turbine
w	—	Water

Greek

η	—	Efficiency, %
η_{ex}	—	Exergy efficiency, %
η_o	—	Optical efficiency, %

References

- [1] S. Hou, H. Zhang, A hybrid solar desalination process of the multi-effect humidification dehumidification and basin-type unit, *Desalination*, 220 (2008) 552–557.
- [2] M.A. Sharaf Eldean, Design and Simulation of Solar Desalination Systems, Ph.D. Thesis (Philography No. 11114571), 2011.
- [3] A.A. Mabrouk, A.S. Nafey, H.E.S. Fath, Thermoeconomic analysis of some existing desalination processes, *Desalination*, 205 (2007) 354–373.
- [4] A.S. Nafey, H.E.S. Fath, A.A. Mabrouk, Thermoeconomic investigation of multi effect evaporation (MEE) and hybrid multi effect evaporation-multi stage flash (MEE-MSF) systems, *Desalination*, 201 (2006) 241–254.
- [5] A.S. Nafey, H.E.S. Fath, A.A. Mabrouk, A new visual package for design and simulation of desalination processes, *Desalination*, 194 (2006) 281–296.
- [6] A.N. Mabrouk, H.S. Fath, Experimental study of high-performance hybrid NF-MSF by renewable energy, *Desal. Water Treat.*, 51 (2013) 6895–6904.

- [7] A.N. Mabrouk, M. Koc, A. Abdala, Technoeconomic analysis of tri-hybrid reverse osmosis-forward osmosis-multi-stage flash desalination process, *Desal. Water Treat.*, 98 (2017) 1–15.
- [8] B. Milow, E. Zarza, Advanced MED solar desalination plants configurations, costs, future - seven years of experience at the Plataforma Solar de Almeria (Spain), *Desalination*, 108 (1996) 51–58.
- [9] M.A. Darwish, H.K. Abdulrahim, A.S. Hassan, A.A. Mabrouk, PV and CSP solar technologies & desalination: economic analysis, *Desal. Water Treat.*, 57 (2016) 16679–16702.
- [10] G. Iaquaniello, A. Salladini, A.A. Mabrouk, H.E.S. Fath, Concentrating solar power (CSP) system integrated with MED-RO hybrid desalination, *Desalination*, 336 (2014) 121–128.
- [11] M.A. Sharaf, A.S. Nafey, L. Garcia-Rodriguez, Exergy and thermo-economic analyses of a combined solar organic cycle with multi effect distillation (MED) desalination process, *Desalination*, 272 (2011) 135–147.
- [12] M.A. Darwish, F. Al-Juwayhel, H. Abdul Raheim, Multi-effect boiling systems from an energy viewpoint, *Desalination*, 194 (2006) 22–39.
- [13] A.M. El-Nashar, K. Ishii, Abu Dhabi solar distillation plant, *Desalination*, 52 (1985) 217–234.
- [14] I.B. Askari, M. Ameri, F. Calise, Energy, exergy and exergoeconomic analysis of different water desalination technologies powered by linear Fresnel solar field, *Desalination*, 425 (2018) 37–67.
- [15] I.B. Askari, M. Ameri, Solar Rankine cycle (SRC) powered by linear Fresnel solar field and integrated with multi effect desalination (MED) system, *Renewable Energy*, 117 (2018) 52–70.
- [16] M. Alhaj, A. Mabrouk, S.G. Al Ghamdi, Energy efficient multi-effect distillation powered by a solar linear Fresnel collector, *Energy Convers. Manage.*, 171 (2018) 576–586.
- [17] V. Samson, R. Packiaraj, R. Velraj, P. Jalihal, Transient analysis of steam accumulator integrated with solar based MED-TVC system, *Desalination*, 435 (2018) 3–22.
- [18] S. Casimiro, J. Cardoso, C. Ioakimidis, J. Farinha Mendes, C. Mineo, A. Cipollina, MED parallel system powered by concentrating solar power (CSP). Model and case study: Trapani, Sicily, *Desal. Water Treat.*, 55 (2015) 3253–3266.
- [19] P. Bandelier, F. Pelascini, J.-J. d'Hurlaborde, A. Maise, B. Boillot, J. Laugier, MED seawater desalination using a low-grade solar heat source, *Desal. Water Treat.*, 57 (2016) 23074–23084.
- [20] L. Yang, T. Shen, B. Zhang, S. Shen, K. Zhang, Exergy analysis of a solar-assisted MED desalination experimental unit, *Desal. Water Treat.*, 51 (2013) 1272–1278.
- [21] P. Palenzuela, D.C. Alarcón-Padilla, G. Zaragoza, Experimental parametric analysis of a solar pilot-scale multi-effect distillation plant, *Desal. Water Treat.*, 57 (2016) 23097–23109.
- [22] M.A. Sharaf, Thermo-economic comparisons of different types of solar desalination processes, *J. Solar Energy Eng.*, 134 (2012) 1–10.
- [23] A.S. Nafey, M.A. Sharaf, L. Garcia-Rodriguez, A new visual library for design and simulation of solar desalination systems (SDS), *Desalination*, 259 (2010) 197–207.
- [24] M.A. Sharaf Eldean, A.M. Soliman, A new visual library for modeling and simulation of renewable energy desalination systems (REDS), *Desal. Water Treat.*, 51 (2013) 6905–6920.
- [25] P. Iodice, G. Langella, A. Amoresano, Modeling and energetic-exergetic evaluation of a novel screw expander-based direct steam generation solar system, *Appl. Therm. Eng.*, 155 (2019) 82–95.
- [26] P. Iodice, G. Langella, A. Amoresano, Energy performance and numerical optimization of a screw expander-based solar thermal electricity system in a wide range of fluctuating operating conditions, *Int. J. Energy Res.*, 44 (2020) 1858–1874.
- [27] Y. Liang, J. Chen, X. Luo, J. Chen, Z. Yang, Y. Chen, Simultaneous optimization of combined supercritical CO₂ Brayton cycle and organic Rankine cycle integrated with concentrated solar power system, *J. Cleaner Prod.*, 266 (2020) 2–4, doi: 10.1016/j.jclepro.2020.121927.
- [28] J. Oyekale, M. Petrollese, F. Heberle, D. Brüggemann, G. Cau, Exergetic and integrated exergoeconomic assessments of a hybrid solar-biomass organic Rankine cycle cogeneration plant, *Energy Convers. Manage.*, 215 (2020) 2–3, doi: 10.1016/j.enconman.2020.112905.
- [29] J. Oyekale, M. Petrollese, G. Cau, Modified auxiliary exergy costing in advanced exergoeconomic analysis applied to a hybrid solar-biomass organic Rankine cycle plant, *Appl. Energy*, 268 (2020) 3–4, doi: 10.1016/j.apenergy.2020.114888.
- [30] <http://www.mats.enea.it/>
- [31] M. Khamis Mansour, M.A. Qassem, H. Fath, CFD analysis of vapor flow and design improvement in MED evaporation chamber, *Desal. Water Treat.*, 56 (2015) 2023–2036.
- [32] A.-N. Mabrouk, H. Fath, G. Iaquaniello, A. Salladini, Simulation and Design of MED Desalination Plant With Air Cooled Condenser Driven by Concentrated Solar Power, *IDA 2013 World Congress on Desalination and Water Reuse*, China, 2013.
- [33] A.S. Nafey, M.A. Sharaf, L. Garcia-Rodriguez, Thermo-economic analysis of a combined solar organic Rankine cycle-reverse osmosis desalination process with different energy recovery configurations, *Desalination*, 261 (2010) 138–147.
- [34] <https://www.therminol.com>
- [35] S. Eldean, M.A. Rafi, K.M. Soliman, A.M. Performance analysis of different working gases for concentrated solar gas engines: Stirling & Brayton, *Energy Convers. Manage.*, 150 (2017) 651–668.
- [36] M.M. Elsayed, I.S. Taha, J.A. Sabbagh, Design of Solar Thermal Systems, Scientific Publishing Center King Abdulaziz University, Jeddah, 1994, pp. 57–61.
- [37] H.T. El-Dessouky, H.M. Ettouney, Fundamentals of Salt Water Desalination, Kuwait University, Elsevier Science, 2002.
- [38] F. Banat, N. Jwaied, Exergy analysis of desalination by solar-powered membrane distillation units, *Desalination*, 230 (2008) 27–40.
- [39] A.S. Nafey, Design and Simulation of Seawater-Thermal Desalination Plants, Leeds University, Ph. D. Thesis, 1988.
- [40] <https://www.acwapower.com/en/projects/noor-energy-1/>
- [41] M.A.S. Eldean, Design and Simulation of Solar Desalination Systems, Ph.D. Thesis, Suez Canal University, Faculty of Petroleum & Mining Engineering, Bibliography No.: 11114571, 2011.
- [42] <https://celsiuscity.eu/thermal-energy-storage/>
- [43] <https://www.redslibrary.com/product-page/solar-radiation-model>
- [44] A.S. Nafey, M.A. Sharaf, Combined solar organic Rankine cycle with reverse osmosis desalination process: energy, exergy, and cost evaluations, *Renewable Energy*, 35 (2010) 2571–2580.

Appendix-A: Molten Salt thermo-physical properties

Liquid phase specific volume m³/kg:

$$v_l = \frac{1}{(2,090 - 0.636 \times (t + 273.15 - 273.15))} \quad (A1)$$

Density:

$$\rho_l = \frac{1}{v_l} \quad (A2)$$

Liquid phase specific heat kJ/kg°C:

$$C_{p_l} = (1,443 + (0.172 \times (t + 273.15 - 273.15))) \times 10^3 \quad (A3)$$

Liquid phase dynamic viscosity Pa·s:

$$\mu_l = \left(\frac{\left(\frac{22.714 - 0.12 \times (t + 273.15 - 273.15) + 2.281 \times 10^{-4} \times ((t + 273.15 - 273.15)^2)}{1,000} \right) - (1.474 \times 10^{-7} \times ((t + 273.15 - 273.15)^3) / 1,000)}{1,000} \right) \quad (A4)$$

Liquid phase thermal conductivity W/m°C:

$$K_l = 0.443 + 1.9 \times 10^{-4} \times (t + 273.15 - 273.15) \quad (A5)$$

Liquid phase entropy kJ/kg°C:

$$S_l = (1,396.0182 \times \log(t + 273.15) + 0.172 \times (t + 273.15)) / 1,000 \quad (A6)$$

Appendix-B: Therminol-VP1 thermo-physical properties [43]

Specific heat capacity, kJ/kg°C:

$$C_p = -0.6622 \times \exp^{(0.001186 \times T)} + 2.178 \times \exp^{(0.0007637 \times T)} \quad (A7)$$

Pressure, bar:

$$P = 1.059e - 9 \times T^4 - 3.412e - 7 \times T^3 + 3.867e - 5 \times T^2 - 0.001491 \times T + 0.01249 \quad (A8)$$

Specific enthalpy, kJ/kg:

$$h = 0.00137 \times T^2 + 1.5 \times T - 18.46 \quad (A9)$$

Specific entropy, kJ/kg°C:

$$S = 1.038 \times \exp^{(0.002218 \times T)} - 0.7889 \times \exp^{(-0.004717 \times T)} \quad (A10)$$

Appendix-C: Toluene thermo-physical properties [44]

Density for liquid and vapor phases kg/m³:

$$\rho_{ll} = -7.981^{-19} \times T^9 + 7.002^{-16} \times T^8 - 2.087^{-13} \times T^7 + 1.821^{-11} \times T^6 + 1.971^{-9} \times T^5 - 3.474^{-7} \times T^4 - 3.29^{-6} \times T^3 + 0.001316 \times T^2 - 0.9326 \times T + 884.5 \quad (A11)$$

$$\rho_{lv} = 7.873^{15} \times \exp^{-((T_{\infty} - 868.2) / 97.11)^2} + 1,898 \times \exp^{-((T_{\infty} - 666.7) / 219.2)^2} \quad (A12)$$

Dynamic viscosity for liquid and vapor phases kg/m³:

$$\mu_{ll} = 10^{-6} \times \left(\frac{3.262729 \times 10^{-5} \times T^3 + 5.14015 \times 10^{-2} \times T^2}{-27.89675 \times T + 5.305598 \times 10^3} \right) \quad (A13)$$

$$\mu_{lv} = 10^{-6} \times \left(\frac{6.338982 \times 10^{-8} \times T^4 - 1.602562 \times 10^{-4} \times T^3 + 1.519286 \times 10^{-1} \times T^2 \dots - 63.99838 \times T + 1.011961 \times 10^4}{1.011961 \times 10^4} \right) \quad (A14)$$

Specific enthalpy of dry saturated vapor kJ/kg

$$h_v = 2.323e - 0.19 \times T^9 + 2.638e - 16 \times T^8 - 7.835e - 14 \times T^7 + 6.784e - 12 \times T^6 + 7.627e - 10 \times T^5 - 1.392e - 7 \times T^4 - 1.443e - 6 \times T^3 + 0.002331 \times T^2 + 1.019 \times T + 490.4 \quad (A15)$$

Specific enthalpy of saturated liquid kJ/kg:

$$h_l = -3.023e - 19 \times T^9 - 2.041e - 16 \times T^8 + 6.098e - 14 \times T^7 - 5.372e - 12 \times T^6 - 5.526e - 10 \times T^5 + 9.276e - 8 \times T^4 + 2.962e - 6 \times T^3 + 0.001018 \times T^2 + 1.628 \times T + 63.19 \quad (A16)$$

Specific entropy of saturated vapor kJ/kg°C:

$$s_v = -6.571e - 16 \times T^6 - 7.761e - 14 \times T^5 + 2.712e - 10 \times T^4 - 1.128e - 7 \times T^3 + 2.61e - 5 \times T^2 - 0.001973 \times T + 1.813 \quad (A17)$$

Specific entropy of saturated liquid kJ/kg°C:

$$s_l = 1.038 \times \exp^{(0.002218 \times T)} - 0.7889 \times \exp^{(-0.004717 \times T)} \quad (A18)$$

Saturation pressure bar:

$$P_{sat} = 7.025e - 22 \times T^9 - 4.53e - 19 \times T^8 + 1.187e - 16 \times T^7 - 2.775e - 14 \times T^6 + 6.104e - 12 \times T^5 + 2.474e - 9 \times T^4 + 2.434e - 7 \times T^3 + 1.429e - 5 \times T^2 + 0.0005795 \times T + 0.009935 \quad (A19)$$